Journal of
Nonlinear Science

Check for updates

Algae–Bacteria Interactions with Nutrients and Light: A Reaction–Diffusion–Advection Model

Yawen Yan[1,2] · **Jimin Zhang**[1] · **Hao Wang**[3]

Abstract

In a poorly mixed water column, a reaction–diffusion–advection system is proposed to model algae–bacteria interactions containing nutrients and light. The basic ecological reproductive indices for the invasion of algae and bacteria into aquatic ecosystems are rigorously derived. All possibilities for the survival or extinction of algae and bacteria are obtained by analyzing nonnegative steady-state solutions. We further explore the influence of spatial factors and abiotic factors on algal or bacterial dynamics. Our results show that bacteria effectively reduce the biomass of algae and prevent them from moving to the water surface and ultimately reduce the probability of harmful algal blooms.

✉ Hao Wang
  hao8@ualberta.ca

1   School of Mathematical Sciences, Heilongjiang University, Harbin 150080, Heilongjiang, People's Republic of China

2   College of Mathematical Sciences, Harbin Engineering University, Harbin 150001, Heilongjiang, People's Republic of China

3   Department of Mathematical and Statistical Sciences, University of Alberta, Edmonton, AB T6G 2G1, Canada

---

⚫ Springer

1 Introduction

Algae form the trophic basis of most aquatic ecosystems and widely distribute over lakes, rivers, and oceans. They generate organic carbon through photosynthesis and consume nutrients such as phosphorus and nitrogen (Huisman et al. 2006; Klausmeier and Litchman 2001; Yoshiyama et al. 2009). As a key component of any aquatic community, bacteria play an important role in degrading organic matter and protecting water quality (Chang et al. 2021; Codeço and Grover 2001; Kong et al. 2018; Wang et al. 2007; Yan et al. 2022). The degradation of bacteria can convert complex organic compounds into inorganic substances, and maintain a sustainable cycle of aquatic ecosystems.

The relationship between algae and bacteria is complicated (see Fig. 1). Algae consume light energy and nutrients (Huisman et al. 2006; Klausmeier and Litchman 2001; Zhang et al. 2021a), and release organic carbon in usable forms for an ecosystem (Medina-Sánchez et al. 2004; Wang et al. 2007; Yan et al. 2022). The bacterial growth depends on nutrients and organic carbon (Crane and Grover 2010; Kong et al. 2018; Medina-Sánchez et al. 2004; Wang et al. 2007). This shows that algae have a bottom-up control on bacteria through released organic carbon. At the same time, algae compete with bacteria for nutrients. Therefore, algae and bacteria influence each other's growth, biomass density, and spatial distribution through the bottom-up control and competition.

The movement of algae and bacteria is mainly caused by turbulence in water. They move around in the water column with turbulence. There is increasing recognition that turbulence intensity changes over water depth and season (Wüest and Lorke 2003; Yoshiyama et al. 2009; Zhang et al. 2021a). Generally speaking, turbulence intensity is stronger in epilimnion or in winter, but weaker in hypolimnion or in summer. When turbulence intensity is relatively weak, it forms a poorly mixed water column. As a consequence, water substances (e.g., nutrients and organic carbon) and aquatic organisms
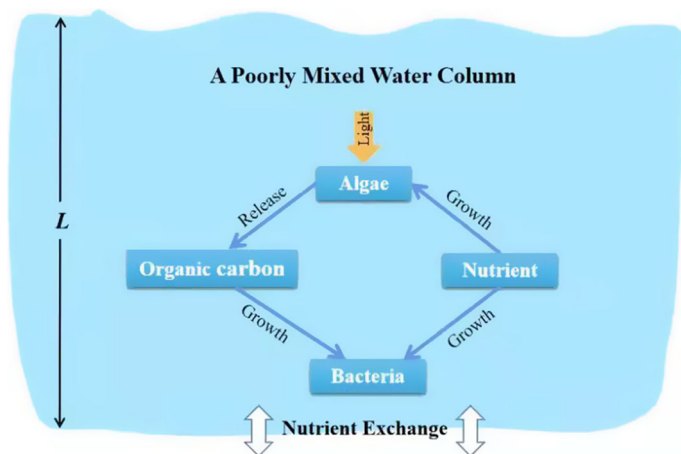
Fig. 1 Algae–bacteria interactions

(e.g., algae and bacteria) exhibit high heterogeneity in a poorly mixed water column. Algae additionally have directional movement containing sinking or buoyant due to gravity or floating up for more light absorption, respectively. This generates the extra advection term in algal equation. Several mathematical models have been proposed to study algal growth in a poorly mixed aquatic environment (Huisman et al. 2006; Jäger et al. 2010; Klausmeier and Litchman 2001; Ryabov et al. 2010; Yoshiyama et al. 2009).

Wang et al. (2007) proposed a stoichiometric bacteria–algae interaction model in the epilimnion. They stated that severe nutrient limitation affects the composition and structure of bacteria in the epilimnion. In Crane and Grover (2010), Edwards (2019), and Yan et al. (2022), the authors considered the predation effect of mixotrophic algae on bacteria based on stoichiometric theory. These algae–bacteria interaction models were proposed for a well-mixed aquatic environment. To our knowledge, there is no existing model that considers algae–bacteria interactions in a poorly mixed aquatic reservoir. Hence, it has great significance to mechanistically establish an algae–bacteria interaction model in a poorly mixed aquatic environment. This is the original motivation of our paper here.

In this study, we consider the algae–bacteria interactions with nutrients and light in a poorly mixed water column by using a reaction–diffusion–advection system. Here we assume that the algal growth needs nutrients and light. Generally, light enters water from its surface and is absorbed by algae and water. Light intensity gradually descends over water depth following the Lambert–Beer's law (Du and Hsu 2010; Hsu and Lou 2010; Huisman and Weissing 1994; Klausmeier and Litchman 2001; Yoshiyama et al. 2009). Nutrients from the water bottom are transported by turbulence to the whole aquatic ecosystem (Klausmeier and Litchman 2001; Zhang et al. 2021a). Bacteria degrade the organic carbon released by algae photosynthesis and consume nutrients. The degradation of bacteria can effectively reduce the organic pollution of aquatic ecosystems. In consideration of the importance of algae and bacteria in aquatic ecosystems, understanding the algae–bacteria interaction mechanism in a poorly mixed aquatic environment is a fundamental ecological problem worth exploring.

Based on the reaction–diffusion–advection model described above, we will establish basic ecological reproductive indices for the invasion of algae and bacteria into aquatic ecosystems. All the possibilities of algae and bacteria from survival to extinction are obtained with rigorous proofs. The vertical distribution and biomass density of algae and bacteria affect the structure and composition of the entire aquatic community. It is noted that algae exhibit complicated vertical distribution and aggregation phenomena in a poorly mixed aquatic environment (Huisman et al. 2006; Klausmeier and Litchman 2001; Ryabov et al. 2010; Yoshiyama et al. 2009; Zhang et al. 2021b). Spatial factors (turbulent diffusion and advection) and abiotic factors (light and nutrients) have significant impacts on the algal biomass density and vertical distribution (Klausmeier and Litchman 2001; Ryabov et al. 2010; Zhang et al. 2021a). Such impacts are thoroughly investigated in this paper. By comparing the changes of algal vertical distribution and biomass in the persistence or extinction of bacteria, we will reveal the important role of bacteria in harmful algal blooms.

The structure of the paper is as follows. In the next section, a reaction–diffusion–advection model describing algae–bacteria interactions is derived for a poorly mixed water column. In Sect. 3, we study dynamical properties of the model including the dissipation and nonnegative steady-state solutions. In Sect. 4, according to realistic ecologically reasonable parameters (see Table 2), we explore the influence of spatial and abiotic factors on the algal or bacterial biomass density and vertical distribution, and consider the important role of bacteria in this process. Finally, we conclude the paper by providing a brief summary and future research questions.

2 Model Formulation

We mechanistically formulate a reaction–diffusion–advection model for algae–bacteria interactions. The biological descriptions of variables and parameters in the model are listed in Table 1. Here the aquatic environment is a poorly mixed water column that has weak turbulence and is relatively undisturbed (Huisman et al. 2006; Klausmeier and Litchman 2001; Wüest and Lorke 2003; Yoshiyama et al. 2009; Zhang et al. 2021b). Denote the independent variables x as the water depth and t as time. The locations $x = 0$ and $x = L$ are the water surface and the water benthos, respectively. This model has four state variables: algal biomass density $A(x, t)$, heterotrophic bacterial biomass density $B(x, t)$, dissolved nutrient concentration $N(x, t)$, and dissolved organic carbon concentration $C(x, t)$.

Algal transport is mainly affected by two kinds of movements. One type is random movement caused by turbulence with a diffusion rate D_a (Huisman et al. 2006; Klausmeier and Litchman 2001; Ryabov et al. 2010). The other type is directional movement with a velocity v containing sinking or buoyant (Grover 2017; Klausmeier and Litchman 2001). Under normal circumstances, algae should sink as a result of gravity ($v > 0$). To absorb more light, algae can move up by generating pseudo vacuoles or storing light density lipids ($v < 0$) (Grover 2017; Klausmeier and Litchman 2001). Algae can also float in the water without directional movement ($v = 0$).

Algal growth mainly has two limiting factors: dissolved nutrient concentration $N(x, t)$ and light intensity I. The algal growth function takes the multiplication of the two (Heggerud et al. 2020; Jäger et al. 2010; Wang et al. 2007; Zhang et al. 2021a), $r_a g(N) f(I(x, A))$, as a smooth approximation of the Liebig's law of minimum. At each depth x, the light intensity I is described as (the Lambert–Beer's law Huisman and Weissing 1994)

$$I(x, A) = I_{in} \exp \left(-k \int_0^x A(s, t)ds - K_{bg}x \right).$$

The functions f and g take (Jäger et al. 2010; Klausmeier and Litchman 2001; Wang et al. 2007)

$$f(I) = \frac{I}{I + \gamma} \ \text{ and } \ g(N) = \frac{N}{N + \beta}.$$

Table 1 Variables and parameters in model (2.5) with biological descriptions

Symbol	Meaning	Symbol	Meaning
x	Water depth	t	Time
A	Algal biomass density	B	Bacterial biomass density
N	Dissolved nutrient concentration	C	Dissolved organic carbon concentration
D_a	Algal vertical turbulent diffusivity	D_b	Bacterial vertical turbulent diffusivity
D_n	Vertical turbulent diffusivity of dissolved nutrients	D_c	Vertical turbulent diffusivity of dissolved organic carbon
v	Algal sinking or buoyant velocity	r_a	Algal maximum production rate
r_b	Maximum bacterial growth rate	L	Depth of the water column
γ	Half-saturation constant for light-limited production of algae	β	Half-saturation constant for nutrient-limited production of algae
I_{in}	The water surface light intensity	K_{bg}	Background light attenuation coefficient
k	Algal light attenuation coefficient	α	Natural degradation rate of bacteria
δ	C-dependent yield constant for bacterial growth	η_n	Half-saturation constant for nutrient-limited production of bacteria
η_c	Half-saturation constant for organic carbon-limited production of bacteria	m_a, m_b	Loss rates of algae and bacteria, respectively
c_a	Average cell quota of algae	c_b	Nutrient to carbon quota of bacteria
a	Nutrient exchange rate	N_b	Dissolved nutrient input concentration

The reduction of algal biomass density is $m_a A$ due to respiration and grazing. At $x = 0$ and $x = L$, we assume no-flux boundary conditions for algae (Hsu and Lou 2010; Huisman et al. 2006; Klausmeier and Litchman 2001). The boundary conditions indicate that algae cannot pass through the water bottom interface and the air–water interface. According to the above assumptions, the algal model is given by

$$
\begin{aligned}
\frac{\partial A(x,t)}{\partial t} &= \text{diffusion} - \text{advection} + \text{algal growth} - \text{algal loss} \\
&= D_a \frac{\partial^2 A}{\partial x^2} - v \frac{\partial A}{\partial x} + r_a g(N) f(I(x,A))A - m_a A, \ x \in (0, L), \\
&\quad D_a A_x(0,t) - vA(0,t) = D_a A_x(L,t) - vA(L,t) = 0.
\end{aligned}
\tag{2.1}
$$

The bacterial transport is controlled by turbulence with a diffusion rate D_b. Bacteria consume organic carbon and dissolved nutrients (Wang et al. 2007; Yan et al. 2022). Then, its growth function is

$$g_b(N, C) = \frac{N}{\eta_n + N} \frac{C}{\eta_c + C}.$$

The bacterial loss rate is m_b due to death, respiration and grazing. Neumann boundary conditions at the two boundaries of the water column state that no bacteria enter or leave the water column. The bacterial model is described as

$$
\begin{aligned}
\frac{\partial B(x, t)}{\partial t} &= \text{diffusion} + \text{bacterial growth} - \text{bacterial loss} \\
&= D_b \frac{\partial^2 B}{\partial x^2} + r_b g_b(N, C)B - m_b B, \; x \in (0, L), \\
B_x(0, t) &= B_x(L, t) = 0.
\end{aligned}
\tag{2.2}
$$

There is a fixed nutrient input concentration N_b at $x = L$ with a nutrient exchange rate a (Klausmeier and Litchman 2001; Yoshiyama et al. 2009). We assume no nutrient input at $x = 0$ (Huisman et al. 2006; Klausmeier and Litchman 2001; Yoshiyama et al. 2009). The dissolved nutrients are transmitted to the whole water column through turbulence with a diffusion rate D_n. The reduction of nutrients consists of two parts: algal consumption with $c_a r_a g(N) f(I(x, A))A$ and bacterial consumption with $c_b r_b g_b(N, C)B$. The dissolved nutrient equation is expressed as

$$
\begin{aligned}
\frac{\partial N(x, t)}{\partial t} &= \text{diffusion} - \text{algal consumption} - \text{bacterial consumption} \\
&= D_n \frac{\partial^2 N}{\partial x^2} - c_a r_a g(N) f(I(x, A))A \\
&\quad - c_b r_b g_b(N, C)B, \; x \in (0, L), \\
N_x(0, t) &= 0, \; D_n N_x(L, t) = a(N_b - N(L, t)) \text{ (nutrients exchange).}
\end{aligned}
\tag{2.3}
$$

The function $C(x, t)$ characterizes the dissolved organic carbon concentration. Its input comes from the exudation of algal photosynthesis in the water column (Medina-Sánchez et al. 2004; Wang et al. 2007; Yan et al. 2022), expressed as $r_a(1 - g(N))f(I(x, A))$. The reduction of organic carbon contains the consumption of bacteria with $(1/\delta)r_b g_b(N, C)B$ and natural degradation αC with a degradation rate α. The transport of dissolved organic carbon is governed by turbulence with a diffusion rate D_c. We also assume Neumann boundary conditions for organic carbon. Then, the dissolved organic carbon equation is

$$
\begin{aligned}
\frac{\partial C(x, t)}{\partial t} &= \text{diffusion} + \text{exudation from algae photosynthesis} \\
&\quad - \text{consumption by bacteria} - \text{natural degradation} \\
&= D_c \frac{\partial^2 C}{\partial x^2} + r_a(1 - g(N))f(I(x, A))A \\
&\quad - \frac{1}{\delta} r_b g_b(N, C)B - \alpha C, x \in (0, L), C_x(0, t) = C_x(L, t) = 0.
\end{aligned}
\tag{2.4}
$$

Coupling equations (2.1)–(2.4), we obtain the complete stoichiometric model for algae–bacteria interactions:

$$
\begin{cases}
\dfrac{\partial A(x,t)}{\partial t} = D_a \dfrac{\partial^2 A}{\partial x^2} - v \dfrac{\partial A}{\partial x} \\
\qquad\quad + r_a g(N) f(I(x,A)) A - m_a A, & x \in (0, L),\ t > 0, \\[6pt]
\dfrac{\partial B(x,t)}{\partial t} = D_b \dfrac{\partial^2 B}{\partial x^2} \\
\qquad\quad + r_b g_b(N, C) B - m_b B, & x \in (0, L),\ t > 0, \\[6pt]
\dfrac{\partial N(x,t)}{\partial t} = D_n \dfrac{\partial^2 N}{\partial x^2} - c_a r_a g(N) f(I(x,A)) A \\
\qquad\quad - c_b r_b g_b(N, C) B, & x \in (0, L),\ t > 0, \\[6pt]
\dfrac{\partial C(x,t)}{\partial t} = D_c \dfrac{\partial^2 C}{\partial x^2} + r_a (1 - g(N)) f(I(x,A)) A \\
\qquad\quad - \dfrac{1}{\delta} r_b g_b(N, C) B - \alpha C, & x \in (0, L),\ t > 0, \\[6pt]
D_a A_x(0,t) - v A(0,t) = D_a A_x(L,t) - v A(L,t) = 0, & t > 0, \\[4pt]
B_x(0,t) = B_x(L,t) = 0, & t > 0, \\[4pt]
N_x(0,t) = 0,\ D_n N_x(L,t) = a(N_b - N(L,t)), & t > 0, \\[4pt]
C_x(0,t) = C_x(L,t) = 0, & t > 0.
\end{cases}
\tag{2.5}
$$

The biologically relevant initial conditions of model (2.5) are

$$
\begin{aligned}
A(x,0) = A_0(x) \geq\not\equiv 0,\ B(x,0) = B_0(x) \geq\not\equiv 0, \\
N(x,0) = N_0(x) \geq\not\equiv 0,\ C(x,0) = C_0(x) \geq\not\equiv 0,
\end{aligned}
\tag{2.6}
$$

for all $x \in [0, L]$. All model parameters except $v \in \mathbb{R}$ are positive constants.

Model (2.5) contains several partial differential equations with advection and nonlocal terms, which make rigorous analysis more challenging. Following standard logics, we show that (2.5) has a unique global nonnegative classical solution $(A(x,t), B(x,t), N(x,t), C(x,t))$ for the initial values satisfying (2.6). In order to describe the algae–bacteria interactions under the influence of nutrients and light, we rigorously analyze dissipation of the solutions and nonnegative steady states of model (2.5).

3 Model Analysis

We explore dynamical properties of model (2.5) containing dissipation of the solutions and nonnegative steady-state solutions.

3.1 Dissipation

The following conclusion assures the dissipation of the solutions of model (2.5).

Theorem 3.1 *The system* (2.5) *is dissipative.*

Proof From the N equation of (2.5), we have

$$\frac{\partial N(x,t)}{\partial t} \leq D_n \frac{\partial^2 N}{\partial x^2},$$
$$N_x(0,t) = 0, \; D_n N_x(L,t) = a(N_b - N(L,t)).$$

Using the comparison theorem of parabolic systems leads to

$$\limsup_{t \to \infty} N(x,t) \leq N_b \text{ on } [0,L]. \tag{3.1}$$

By using the similar methods and arguments of Lemma 3.2 in (Du and Hsu 2010) and Lemma 2.1 in Mei and Wang (2021), A is uniformly bounded and ultimately bounded. Then, we can find a $\theta > 0$ satisfying

$$A(x,t) \leq \theta \text{ on } [0,L], \; t > 0.$$

From the C equation of (2.5), we obtain

$$\frac{\partial C(x,t)}{\partial t} \leq D_c \frac{\partial^2 C}{\partial x^2} + r_a \theta f(I_{in}) - \alpha C,$$
$$C_x(0,t) = C_x(L,t) = 0.$$

Hence,

$$\limsup_{t \to \infty} C(x,t) \leq \frac{r_a \theta f(I_{in})}{\alpha} \text{ on } [0,L].$$

We next show that B is ultimately bounded. Multiplying both sides of the B equation of (2.5) by $1/\delta$, and then adding the C equation of (2.5), we obtain

$$\frac{\partial((1/\delta)B + C)}{\partial t} = \frac{D_b}{\delta}\frac{\partial^2 B}{\partial x^2} + D_c\frac{\partial^2 C}{\partial x^2} + r_a(1 - g(N))f(I(x,A))A - \frac{m_b}{\delta}B - \alpha C$$
$$B_x(0,t) = B_x(L,t) = 0, \; C_x(0,t) = C_x(L,t) = 0.$$

Integrating over $[0,L]$ gives

$$\left(\int_0^L \left(\frac{1}{\delta}B + C\right)(x,t)\mathrm{d}x\right)_t \leq r_a \theta L f(I_{in})$$
$$- \min\{m_b, \alpha\} \int_0^L \left(\frac{1}{\delta}B + C\right)(x,t)\mathrm{d}x.$$

Hence,

$$\frac{1}{\delta} \int_0^L B(x,t)\mathrm{d}x \leq \int_0^L \left(\frac{1}{\delta}B + C\right)(x,t)\mathrm{d}x$$
$$\leq \frac{r_a\theta Lf(I_{in})}{\min\{m_b,\alpha\}} + e^{-\min\{m_b,\alpha\}t}\int_0^L \left(\frac{1}{\delta}B_0 + C_0\right)(x)\mathrm{d}x. \tag{3.2}$$

Assume that B is not ultimately bounded. Let $H(t) := \max_{x\in[0,L],\tau\in[0,t]} B(x,\tau)$. Then, $H(t)$ is increasing for t and there exists a strictly monotone increasing sequence $\{t_i\}_{i=1}^\infty$ such that $H(t_i) = \max_{x\in[0,L]} B(x,t_i) \to \infty$ as $i \to \infty$. We choose $t_1 > 1$ and denote

$$\pi_i(x,t) = B(x,t+t_i-1)/H(t_i),$$
$$r_i(x,t) = r_b g_b(N(x,t+t_i-1), C(x,t+t_i-1)) - m_b.$$

A direct calculation obtains

$$\frac{\partial \pi_i}{\partial t} = D_b\frac{\partial^2 \pi_i}{\partial x^2} + r_i(x,t)\pi_i, \; x \in (0,L), \; t > 0,$$
$$(\pi_i)_x(0,t) = (\pi_i)_x(L,t) = 0, \; t > 0,$$
$$0 \leq \pi_i(x,0) \leq 1, \; x \in [0,L].$$

Note that $|r_i(x,t)| \leq r_b + m_b$ on $[0,L]$ for $t \geq 0$. Thus,

$$0 \leq \pi_i(x,t) \leq e^{(r_b+m_b)t}, \; x \in [0,L], \; t \geq 0.$$

According to the standard parabolic regularity, $\{\pi_i\}$ is bounded in $C^{1+\omega,\omega}([0,L] \times [1/3,3])$ for any $\omega \in (0,1)$. Then, we assume $\pi_i \to \pi^*$ in $C^{1,0}([0,L] \times [1/3,3])$ as $i \to \infty$. Similarly, $r_i \to r^*$ weakly in $L^2([0,L] \times [1/3,3])$ as $i \to \infty$ and $|r^*| \leq r_b + m_b$. Hence, π^* satisfies

$$\frac{\partial \pi^*}{\partial t} = D_b\frac{\partial^2 \pi^*}{\partial x^2} + r^*(x,t)\pi_i^*, \; x \in (0,L), \; t \in [1/3,3],$$
$$(\pi^*)_x(0,t) = (\pi^*)_x(L,t) = 0, \; t \in [1/3,3],$$
$$0 \leq \pi^*(x,0) \leq e^{3(r_b+m_b)}, \; x \in [0,L].$$

From $\max_{x\in[0,L]} \pi_i(x,1) = 1$, $\max_{x\in[0,L]} \pi^*(x,1) = 1$ and then $\pi^* \geq \not\equiv 0$. It follows from the strong maximum principle that there exists $\kappa_0 > 0$ such that $\pi^*(x,1) \geq \kappa_0 > 0$ on $[0,L]$. This implies that $\pi_i(x,1) \geq \kappa_0/2 > 0$ on $[0,L]$ if i is sufficiently large. Then, $B(x,t_i) \geq (\kappa_0/2)H(t_i)$ for all $x \in [0,L]$ and sufficiently large i. This shows

$$\int_0^L B(x,t_i)\mathrm{d}x \geq \frac{\kappa_0 L}{2}H(t_i) \to \infty \text{ as } i \to \infty.$$

It is a contradiction to (3.2). Therefore, B is ultimately bounded. This completes the proof. $\square$

Let

$$\mathbb{Y} := \{(u_1, u_2, u_3, u_4) \in C([0, L], \mathbb{R}^4) : u_i(x) \geq 0 \text{ on } [0, L], \ i = 1, 2, 3, 4\}. \tag{3.3}$$

The system (2.5) generates a semiflow $\Pi(t) : \mathbb{Y} \to \mathbb{Y}$ by

$$\Pi(t)(u_0)(x) = (A(x, t, u_0), B(x, t, u_0), N(x, t, u_0), C(x, t, u_0)), \ x \in [0, L], \ t \geq 0,$$

where $u_0 = (A_0, B_0, N_0, C_0) \in \mathbb{Y}$. By Theorem 3.1, $\Pi(t)$ is point dissipative. Notice that $\Pi(t)$ is also compact, we conclude that $\Pi(t) : \mathbb{Y} \to \mathbb{Y}$ has a global compact attractor in $\mathbb{Y}$ (see Theorem 3.4.8 in Hale 1988).

3.2 Semi-trivial Steady States

Model (2.5) has two semi-trivial steady states as follows:

1. Nutrient-only semi-trivial steady state $E_1 = (0, 0, N_b, 0)$.
2. Algae–nutrient–organic carbon semi-trivial steady state $E_2 = (A_2(x), 0, N_2(x), C_2(x))$, where $A_2(x), N_2(x), C_2(x)$ satisfy

$$\begin{cases} D_a A'' - v A' + (r_a g(N) f(I(x, A)) - m_a)A = 0, & x \in (0, L), \\ D_n N'' - c_a r_a g(N) f(I(x, A))A = 0, & x \in (0, L), \\ D_c C'' + r_a(1 - g(N)) f(I(x, A))A - \alpha C = 0, & x \in (0, L), \\ D_a A'(0) - v A(0) = D_a A'(L) - v A(L) = 0, \\ N'(0) = 0, D_n N'(L) = a(N_b - N(L)), \\ C'(0) = C'(L) = 0. \end{cases} \tag{3.4}$$

To facilitate the following discussion, for $p \in L^\infty([0, L])$, we let $\lambda_1(p(x), D, v, L)$ denote the principal eigenvalue of

$$\begin{cases} D\psi''(x) - v\psi'(x) + p(x)\psi = \lambda\psi, & x \in (0, L), \\ D\psi'(0) - v\psi(0) = D\psi'(L) - v\psi(L) = 0. \end{cases} \tag{3.5}$$

If $v = 0$, then $\lambda_1(p(x), D, 0, L) = \lambda_1(p(x), D, L)$. It follows from Proposition 3.1 in Wang et al. (2019) that the principal eigenvalue $\lambda_1(p(x), D, v, L)$ of (3.5) exists and is unique, and $\lambda_1(p_1(x), D, v, L) \geq \lambda_1(p_2(x), D, v, L)$ if $p_1(x) \geq p_2(x)$. We define the following basic ecological reproductive indices for algae and bacteria:

$$R_a = \frac{m_a^*}{m_a}, \quad R_b = \frac{m_b^*}{m_b}, \tag{3.6}$$

where

$$m_a^* = \lambda_1(r_a g(N_b) f(I(x,0)), D_a, v, L), \quad m_b^* = \lambda_1(r_b g_b(N_2(x), C_2(x)), D_b, L).$$

Here, R_a (or R_b) is an indicator to measure the viability of algae (or bacteria). It characterizes the average number of new algae (or bacteria) produced by one cubic meter of algae (or bacteria) in a life cycle of algae (or bacteria). In the following discussion, we show that $R_a = 1$ and $R_b = 1$ are critical values for algae and bacteria to invade aquatic ecosystems.

Theorem 3.2 *Model* (2.5) *has a unique* $E_1 \equiv (0, 0, N_b, 0)$. *If* $R_a < 1$, *then* E_1 *is globally asymptotically stable, while* E_1 *is unstable if* $R_a > 1$.

Proof It follows from (2.5) that $E_1 = (0, 0, N_b, 0)$ exists and it is unique. The local stability of E_1 is obtained by

$$\lambda\zeta(x) = D_a \zeta''(x) - v\zeta'(x) + (r_a g(N_b) f(I(x,0)) - m_a)\zeta(x), \quad x \in (0, L), \quad (3.7a)$$
$$\lambda\phi(x) = D_b \phi''(x) - m_b \phi(x), \quad x \in (0, L), \quad (3.7b)$$
$$\lambda\varphi(x) = D_n \varphi''(x) - c_a r_a g(N_b) f(I(x,0))\zeta(x), \quad x \in (0, L), \quad (3.7c)$$
$$\lambda\psi(x) = D_c \psi''(x) + r_a(1 - g(N_b)) f(I(x,0))\zeta(x) - \alpha\psi(x), \quad x \in (0, L), \quad (3.7d)$$
$$D_a \zeta'(0) - v\zeta(0) = D_a \zeta'(L) - v\zeta(L) = 0, \quad (3.7e)$$
$$\phi'(0) = \phi'(L) = 0, \quad (3.7f)$$
$$\varphi'(0) = 0, \quad D_n \varphi'(L) = -a\varphi(L), \quad (3.7g)$$
$$\psi'(0) = \psi'(L) = 0. \quad (3.7h)$$

To obtain the local stability of E_1, we let $\lambda_{\max}$ be the largest eigenvalue of (3.7) and $(\zeta, \phi, \varphi, \psi)$ be the corresponding eigenfunction. Since (3.7) is partially decoupled, we explore two cases: (i) $\zeta \neq 0$ and (ii) $\zeta \equiv 0$.

Case (i): $\zeta \neq 0$. In this case, (3.7a) and its boundary condition (3.7e) determine the stability of E_1. It is clear that its principal eigenvalue is $\lambda_1(r_a g(N_b) f(I(x,0)) - m_a, D_a, v, L) = m_a^* - m_a < 0$ with $(\zeta, \phi, \varphi, \psi)$, where ζ is the principal eigenvalue function to $m_a^* - m_a$, and (ϕ, φ, ψ) can be solved from (3.7b)–(3.7d) and their boundary conditions (3.7f)–(3.7h).

Case (ii): $\zeta \equiv 0$. In this case, (3.7) reduces to

$$\begin{cases} \lambda\phi(x) = D_b \phi''(x) - m_b \phi(x), \quad x \in (0, L), \quad \phi'(0) = \phi'(L) = 0, \\ \lambda\varphi(x) = D_n \varphi''(x), \quad x \in (0, L), \quad \varphi'(0) = 0, \quad D_n \varphi'(L) = -a\varphi(L), \\ \lambda\psi(x) = D_c \psi''(x) - \alpha\psi(x), \quad x \in (0, L), \quad \psi'(0) = \psi'(L) = 0. \end{cases} \quad (3.8)$$

Note that (3.8) is completely decoupled, and the principal eigenvalue of each equation in (3.8) is negative. Then, $\operatorname{Re} \lambda_{\max} < 0$.

As a result of cases (i) and (ii), if $R_a < 1$, then $\operatorname{Re} \lambda_{\max} < 0$ and E_1 is locally asymptotically stable; conversely, E_1 is unstable if $R_a > 1$.

We will prove that E_1 is globally attractive. For any $\epsilon > 0$, it follows from (3.1) that there exists a $t_1 > 0$ such that $N(x, t) \leq N_b + \epsilon$ on $[0, L]$ for any $t \geq t_1$. Then,

$$\frac{\partial A}{\partial t} \leq D_a \frac{\partial^2 A}{\partial x^2} - v \frac{\partial A}{\partial x} + r_a g(N_b + \epsilon) f(I(x, 0))A - m_a A, \ x \in (0, L), \ t > t_1,$$
$$D_a A_x(0, t) - v A(0, t) = D_a A_x(L, t) - v A(L, t) = 0, \ t > t_1,$$
$$A(x, t_1) = A^*(x), \ x \in [0, L].$$

Let $v(x)$ be an eigenfunction corresponding to $\lambda_1(r_a g(N_b + \epsilon) f(I(x, 0)), D_a, v, L)$ satisfying $A^*(x) \leq cv(x)$ for a sufficiently large c. Then, we obtain

$$A(x, t) \leq ce^{-(m_a - \lambda_1(r_a g(N_b + \epsilon) f(I(x, 0)), D_a, v, L))(t - t_1)} v(x) \text{ for all } t \geq t_1, \ x \in [0, L].$$

Note that ϵ is sufficiently small, $m_a - \lambda_1(r_a g(N_b + \epsilon) f(I(x, 0)), D_a, v, L) > 0$ since $R_a < 1$. Hence, $\limsup_{t \to \infty} A(x, t) = 0$ on $[0, L]$. For the above ϵ, we can find a $t_2 > t_1$ such that $A(x, t) \leq \epsilon$ on $[0, L]$ for any $t \geq t_2$. It follows that

$$\frac{\partial C}{\partial t} \leq D_c \frac{\partial^2 C}{\partial x^2} + r_a f(I_{in}) \epsilon - \alpha C, \ x \in (0, L), \ t > t_2,$$
$$C_x(0, t) = C_x(L, t) = 0, \ t > t_2, \tag{3.9}$$
$$C(x, t_2) = C^*(x), \ x \in [0, L].$$

By using the comparison theorem of parabolic systems, we have $\limsup_{t \to \infty} C(x, t) \leq r_a f(I_{in}) \epsilon / \alpha$ for any $x \in [0, L]$. Then, $\limsup_{t \to \infty} C(x, t) = 0$ on $[0, L]$ since ϵ is sufficiently small. There exists $t_3 > t_2$ such that $C(x, t) \leq \epsilon$ on $[0, L]$ for any $t \geq t_3$. By the second equation of (2.5), we obtain

$$\frac{\partial B}{\partial t} \leq D_b \frac{\partial^2 B}{\partial x^2} + r_b g_b(N_b + \epsilon, \epsilon)B - m_b B, \ x \in (0, L), \ t > t_3,$$
$$B_x(0, t) = B_x(L, t) = 0, \ t > t_3, \tag{3.10}$$
$$B(x, t_3) = B^*(x), \ x \in [0, L].$$

From the continuity of g_b and the sufficient smallness of ϵ, we obtain $r_b g_b(N_b + \epsilon, \epsilon) - m_b < 0$, which leads to $\limsup_{t \to \infty} B(x, t) = 0$ on $[0, L]$. By the theory of asymptotic autonomous systems (see Theorem 1.8 in Mischaikow et al. 1995 or Theorem 4.1 in Thieme 1992), the third equation of (2.5) reduces to

$$\frac{\partial N}{\partial t} = D_n \frac{\partial^2 N}{\partial x^2}, \ x \in (0, L), \ N_x(0, t) = 0,$$
$$D_n N_x(L, t) = a(N_b - N(L, t)), \ t > 0. \tag{3.11}$$

Thus, $N(x, t)$ converges to N_b uniformly on $[0, L]$ as $t \to \infty$. This means that E_1 is globally attractive. Therefore, E_1 is globally asymptotically stable if $R_a < 1$. $\qquad \square$

Remark 3.3 The condition $R_a < 1$ results in the inevitable extinction of algae and bacteria for all initial conditions, but nutrients always exist. The threshold $R_a = 1$ is an indicator for the stability of E_1, and m_a^* provides the threshold loss rate for algae from extinction to persistence. From the expression of R_a, one can observe that it depends on some key environmental factors: vertical turbulent diffusivity D_a, sinking/buoyant velocity v, the light intensity I_{in}, the nutrient concentration N_b, and the water column depth L. This indicates that these environmental factors jointly determine whether algae can successfully invade aquatic ecosystems.

Next, we show the existence of algae–nutrient–organic carbon semi-trivial steady state E_2. We first establish *a priori estimate* for nonnegative solutions $(A_2(x), N_2(x), C_2(x))$ of (3.4).

Lemma 3.4 *Assume that $(A_2(x), N_2(x), C_2(x))$ is a nonnegative solution of (3.4) with $A_2, N_2, C_2 \not\equiv 0$. Then,*

(1) $0 < N_2(x) < N_b$ *for any $x \in [0, L]$ and $0 < m_a < m_a^*$;*
(2) *for any $\varepsilon > 0$, there exists a positive constant $K(\varepsilon)$ such that*

$$0 < A_2(x) \le K(\varepsilon) \text{ and } 0 < C_2(x) \le r_a f(I_{in}) K(\varepsilon) \left(\frac{1}{\alpha} + \frac{2L^2}{D_c} \right)$$

on $[0, L]$ for $m_a \in [\varepsilon, m_a^*)$.

Proof (1) Let $V = e^{-(v/D_a)x} A_2$. From (3.4), we have

$$- D_a V'' - v V' + m_a V = r_a g(N_2) f(I(x, A_2)) V \ge 0, \ x \in (0, L),$$
$$V'(0) = V'(L) = 0.$$

It follows from the strong maximum principle that $V > 0$ and $A_2 > 0$ on $[0, L]$. By (3.4), we have

$$a(N_b - N_2(L)) = \int_0^L c_a r_a g(N_2(x)) f(I(x, A_2(x))) A_2(x) \mathrm{d}x$$
$$= c_a m_a \int_0^L A_2(x) \mathrm{d}x > 0,$$

which implies that $N_2(L) < N_b$. Note that

$$- D_n N_2'' + \left(c_a r_a f(I(x, A_2)) A_2 \int_0^1 g'(s N_2) ds \right) N_2 = 0, \ x \in (0, L),$$
$$- D_c C_2'' + \alpha C_2 = r_a (1 - g(N_2)) f(I(x, A_2)) A_2 \ge 0, \ x \in (0, L)$$

with

$$N_2'(0) = 0, \ D_n N_2'(L) = a(N_b - N_2(L)) > 0, \ C_2'(0) = C_2'(L) = 0.$$

By applying the maximum principle again, $N_2 > 0$ and $C_2 > 0$ on $[0, L]$.

From the equation of N in (3.4) and its boundary condition, we get $N_2''(x) > 0$ and $N_2'(x) > 0$ on $(0, L)$. Hence, $0 < N_2 < N_b$ for any $x \in [0, L]$. For the equation of A in (3.4), we obtain

$$\lambda_1(r_a g(N_2) f(I(x, A_2)), D_a, v, L) = m_a$$

with the corresponding principal eigenfunction A_2. By the monotonicity of principal eigenvalue for the weight functions, we have

$$m_a = \lambda_1(r_a g(N_2) f(I(x, A_2)), D_a, v, L) < \lambda_1(r_a g(N_b) f(I(x, 0)), D_a, v, L) = m_a^*.$$

(2) For fixed $\varepsilon > 0$, we assume that A_2 is not bounded for $m_a \in [\varepsilon, m_a^*)$. This implies that there are a sequence $m_a^i \in [\varepsilon, m_a^*)$ and corresponding positive solutions (A_2^i, N_2^i, C_2^i) such that $\|A_2^i\|_\infty \to \infty$ and $m_a^i \to \hat{m}_a \in [\varepsilon, m_a^*)$ as $i \to \infty$. Let $a_i = A_2^i / \|A_2^i\|_\infty$. It follows from (3.4) that

$$\begin{cases} -D_a a_i'' + v a_i' + m_a^i a_i = r_a g(N_2^i) f(I(x, A_2^i)) a_i, & x \in (0, L), \\ D_a a_i'(0) - v a_i(0) = D_a a_i'(L) - v a_i(L) = 0. \end{cases}$$

Note that $r_a g(N_2^i) f(I(x, A_2^i)) \le r_a$ on $[0, L]$ for any i. Then, $r_a g(N_2^i) f(I(x, A_2^i)) \to l$ weakly in $L^2([0, L])$. From L^p theory of elliptic operators and passing to a subsequence, we have $a_i \to a$ in $W^{2,p}([0, L])$ (or in $C^{1,\alpha}([0, L])$ from Sobolev's embedding) as $i \to \infty$. Therefore, a satisfies (in the weak sense)

$$\begin{cases} -D_a a'' + v a' + \hat{m}_a a = l a, & x \in (0, L), \\ D_a a'(0) - v a(0) = D_a a'(L) - v a(L) = 0. \end{cases} \tag{3.12}$$

Note that $a \ge 0$ with $\|a\|_\infty = 1$. This shows that $a > 0$ on $[0, L]$. On the other hand, $A_2^i = \|A_2^i\|_\infty a_i \to \infty$ uniformly on $[0, L]$ when $i \to \infty$, and thus, $l = 0$. Integrating (3.12) over $[0, L]$ gives $0 = \hat{m}_a \int_0^L a(x) \mathrm{d}x > 0$. It is a contradiction. This shows that there exists a $K(\varepsilon) > 0$ such that $0 < A_2(x) \le K(\varepsilon)$ on $[0, L]$ for all $m_a \in [\varepsilon, m_a^*)$.

From the C equation in (3.4), we obtain

$$\int_0^L C_2(x) \mathrm{d}x \le \frac{r_a f(I_{in})}{\alpha} \int_0^L A_2(x) \mathrm{d}x \le \frac{r_a L f(I_{in}) K(\varepsilon)}{\alpha}.$$

Then,

$$|C_2'(x)| = \left| \int_0^x C_2''(z) \mathrm{d}z \right| = \frac{1}{D_c} \left| \int_0^x (\alpha C - r_a(1 - g(N_2)) f(I(z, A_2)) A_2) \mathrm{d}z \right|$$

$$\le \left| \frac{\alpha}{D_c} \int_0^L C_2(x) \mathrm{d}x + \frac{r_a f(I_{in})}{D_c} \int_0^L A_2(x) \mathrm{d}x \right| \le \frac{2 r_a L f(I_{in}) K(\varepsilon)}{D_c}.$$

Let $C_2(x_0) = \min_{x \in [0,L]} C_2(x)$. Then,

$$C_2(x_0) \leq \frac{1}{L} \int_0^L C_2(x)\mathrm{d}x \leq \frac{r_a f(I_{in})K(\varepsilon)}{\alpha}.$$

For all $x \in [0, L]$, we have

$$|C_2(x)| = |C_2(x_0) + C_2(x) - C_2(x_0)| = |C_2(x_0)| + \left| \int_{x_0}^x C_2'(x)\mathrm{d}x \right|$$

$$\leq r_a f(I_{in})K(\varepsilon)\left(\frac{1}{\alpha} + \frac{2L^2}{D_c} \right).$$

$\square$

We consider the existence of E_2 by using bifurcation theory with m_a as the bifurcation parameter. Let $\mathcal{X} := \mathcal{X}_1 \times \mathcal{X}_2 \times \mathcal{X}_3$ and $\mathcal{Y} := C([0, L])$, where

$$\mathcal{X}_1 := \{p \in C^2([0, L]) : D_a p'(0) - vp(0) = D_a p'(L) - vp(L) = 0\},$$
$$\mathcal{X}_2 := \{p \in C^2([0, L]) : p'(0) = 0\},$$
$$\mathcal{X}_3 := \{p \in C^2([0, L]) : p'(0) = p'(L) = 0\}.$$

Define a nonlinear mapping $H : \mathbb{R}^+ \times \mathcal{X} \to \mathcal{Y}^3 \times \mathbb{R}$ by

$$H(m_a, A, N, C) = \begin{pmatrix} D_a A'' - vA' + r_a g(N)f(I(x, A))A - m_a A \\ D_n N'' - c_a r_a g(N)f(I(x, A))A \\ D_c C'' + r_a(1 - g(N))f(I(x, A))A - \alpha C \\ D_n N'(L) - a(N_b - N(L)) \end{pmatrix}.$$

Let Λ be the set of all positive solutions $(m_a, A, N, C) \in \mathbb{R}^+ \times \mathcal{X}$ of (3.4). We now state the existence of algae–nutrient–organic carbon semi-trivial steady state E_2 for $m_a \in (0, m_a^*)$.

Theorem 3.5 *If $R_a > 1$ holds, then*

(i) *(2.5) has at least one positive algae–nutrient–organic carbon semi-trivial steady-state solution E_2 for $0 < m_a < m_a^*$;*

(ii) *there is a connected component Λ^+ in Λ such that it connects to the line $\Gamma_1 = \{(m_a, 0, N_b, 0) : m_a > 0\}$ and its closure includes $(m_a^*, 0, N_b, 0)$. Moreover, near $(m_a^*, 0, N_b, 0)$, Λ^+ is a smooth curve in a form $\{(m_a(s), A_2(s, x), N_2(s, x), C_2(s, x)) : 0 < s < \bar{\epsilon}\}$ for some $\bar{\epsilon} > 0$ with $m_a'(0) < 0$.*

Proof We first show that E_2 bifurcates from E_1 at $m_a = m_a^*$ by using local bifurcation theory (see Theorem 1.7 in Crandall and Rabinowitz 1971). It is obvious that $H(m_a, 0, N_b, 0) = 0$. Let $J := H_{(A,N,C)}(m_a^*, 0, N_b, 0)$. For any $(\zeta, \varphi, \psi) \in \mathcal{X}$, we

have

$$J[\zeta, \varphi, \psi] = \begin{pmatrix} D_a\zeta'' - v\zeta' + (r_a g(N_b) f(I(x,0)) - m_a^*)\zeta \\ D_n\varphi'' - c_a r_a g(N_b) f(I(x,0))\zeta \\ D_c\psi'' + r_a(1 - g(N_b)) f(I(x,0))\zeta - \alpha\psi \\ D_n\varphi'(L) + a\varphi(L) \end{pmatrix}. \tag{3.13}$$

For $(\zeta_1, \varphi_1, \psi_1) \in \ker J$, we obtain

$$D_a\zeta_1'' - v\zeta_1' + (r_a g(N_b) f(I(x,0)) - m_a^*)\zeta_1 = 0, \ x \in (0, L), \tag{3.14a}$$

$$D_n\varphi_1'' - c_a r_a g(N_b) f(I(x,0))\zeta_1 = 0, \ x \in (0, L), \tag{3.14b}$$

$$D_c\psi_1'' + r_a(1 - g(N_b)) f(I(x,0))\zeta_1 - \alpha\psi_1 = 0, \ x \in (0, L), \tag{3.14c}$$

$$D_n\varphi_1'(L) + a\varphi_1(L) = 0. \tag{3.14d}$$

Note that m_a^* is the principal eigenvalue of (3.5) for $p(x) = r_a g(N_b) f(I(x,0))$. This means that the corresponding positive eigenfunction $\bar{\zeta}$ for m_a^* is the unique solution of (3.14a) if a constant coefficient is not considered. Let $M = \max_{x \in [0,L]} r_a(1 - g(N_b)) f(I(x,0))\bar{\zeta}$. It can be seen that 0 and $(M + 1)/\alpha$ are the lower and upper solutions of (3.14c), respectively. By Theorem 3.2.1 in Pao (1992), (3.14c) has a solution $\bar{\psi}$ satisfying $0 \leq \bar{\psi} \leq (M+1)/\alpha$. From the strong maximum principle, $\bar{\psi} > 0$ for any $x \in [0, L]$, and it is unique since (3.14c) is a linear ODE. We can also conclude that there is a unique function $\bar{\varphi} \in \mathcal{X}_2$ satisfying (3.14b). Hence, dim ker $J = 1$ and ker $J = \text{span}\{(\bar{\zeta}, \bar{\varphi}, \bar{\psi})\}$.

If $(\delta_1, \delta_2, \delta_3, \delta_4) \in \text{range } J$, then there exists $(\zeta_2(x), \varphi_2(x), \psi_2(x)) \in \mathcal{X}$ such that

$$\begin{aligned} D_a\zeta_2'' - v\zeta_2' + (r_a g(N_b) f(I(x,0)) - m_a^*)\zeta_2 &= \delta_1, \ x \in (0, L), \\ D_n\varphi_2'' - c_a r_a g(N_b) f(I(x,0))\zeta_2 &= \delta_2, \ x \in (0, L), \\ D_c\psi_2'' + r_a(1 - g(N_b)) f(I(x,0))\zeta_2 - \alpha\psi_2 &= \delta_3, \ x \in (0, L), \\ D_n\varphi_2'(L) + a\varphi_2(L) &= \delta_4. \end{aligned} \tag{3.15}$$

We multiply (3.14a) and the first equation of (3.15) by $\zeta_2 e^{-(v/D_a)x}$ and $\zeta_1 e^{-(v/D_a)x}$, respectively, and then subtract the multiplications and finally integrate over $[0, L]$ to obtain $\int_0^L \delta_1(x) e^{-(v/D_a)x} \zeta_1(x) dx = 0$. This shows $\int_0^L \delta_1(x) e^{-(v/D_a)x} \bar{\zeta}(x) dx = 0$. By the Fredholm alternative theorem, there exists a unique solution $\varphi_2 \in \mathcal{X}_2$ for any $\zeta_2 \in \mathcal{X}_1$ satisfying the second and fourth equations in (3.15). Similarly, the third equation in (3.15) has a unique solution $\psi_2 \in \mathcal{X}_3$ for any $\zeta_2 \in \mathcal{X}_1$. Then,

$$\text{range } J = \left\{ (\delta_1, \delta_2, \delta_3, \delta_4) \in \mathcal{Y}^3 \times \mathbb{R} : \int_0^L \delta_1(x) e^{-(v/D_a)x} \bar{\zeta}(x) dx = 0 \right\}$$

and codim range $J = 1$. Note that

$$H_{(m_a, (A,N,C))}(m_a^*, 0, N_b, 0)(\bar{\zeta}, \bar{\varphi}, \bar{\psi}) = (-\bar{\zeta}(x), 0, 0, 0).$$

This indicates $H_{(m_a,(A,N,C))}(m_a^*, 0, N_b, 0) \notin$ range J due to $\int_0^L e^{-(v/D_a)x}\bar{\zeta}^2(x)\mathrm{d}x \neq 0$.

From the Crandall–Rabinowitz bifurcation theorem (Theorem 1.7 in Crandall and Rabinowitz (1971)), near $(m_a^*, 0, N_b, 0)$ all positive solutions of (3.4) lie on a smooth curve $\Gamma_2 = \{(m_a(s), A_2(s, x), N_2(s, x), C_2(s, x)) : s \in (0, \bar{\epsilon})\}$ for some $\bar{\epsilon} > 0$ with the form

$$A_2(s, x) = s\bar{\zeta}(x) + o(s), \ N_2(s, x) = N_b + s\bar{\varphi}(x) + o(s),$$
$$C_2(s, x) = s\bar{\psi}(x) + o(s).$$

Define a linear functional μ on $\mathcal{Y}^3 \times \mathbb{R}$ by

$$\langle \mu, (\delta_1, \delta_2, \delta_3, \delta_4) \rangle = \int_0^L \delta_1(x)e^{-(v/D_a)x}\bar{\zeta}(x)\mathrm{d}x.$$

A direct calculation gives

$$
m_a'(0) = -\frac{\langle \mu, H_{(A,N,C)(A,N,C)} \left(m_a^*, 0, N_b, 0 \right) [\bar{\zeta}, \bar{\varphi}, \bar{\psi}]^2 \rangle}{2 \langle \mu, H_{(m_a,(A,N,C))} \left(m_a^*, 0, N_b, 0 \right) [\bar{\zeta}, \bar{\varphi}, \bar{\psi}] \rangle}
$$
$$
= \frac{\displaystyle\int_0^L r_a g(N_b) f(I(x,0))\bar{\zeta}^2 e^{-(v/D_a)x} \upsilon(x, \bar{\zeta}, \bar{\varphi})\mathrm{d}x}{\displaystyle\int_0^L e^{-(v/D_a)x}\bar{\zeta}^2(x)\mathrm{d}x},
$$

where

$$\upsilon(x, \bar{\zeta}, \bar{\varphi}) = -\frac{\gamma k}{I(x,0) + \gamma}\int_0^x \bar{\zeta}(s)ds + \frac{\beta}{N_b(N_b + \beta)}\bar{\varphi}.$$

From (3.14b) and $\bar{\zeta} > 0$ on $[0, L]$, we conclude that $\bar{\varphi}'$ is a strictly increasing function on $[0, L]$. Combining $\bar{\varphi}'(0) = 0$ and (3.14d) leads to $\bar{\varphi}' > 0$ on $[0, L]$ and $\bar{\varphi}(L) < 0$. This means that $\bar{\varphi} < 0$ for all $x \in [0, L]$. Therefore, $m_a'(0) < 0$ and the bifurcation at $(0, N_b, 0)$ is backward. From Theorem 3.3 and Remark 3.4 in Shi and Wang (2009), there exists a connected component Λ^+ of Λ such that Λ^+ connects to Γ_1 and contains Γ_2. Moreover, the closure of Λ^+ includes $(m_a^*, 0, N_b, 0)$. The proof of part (ii) is complete.

Now we turn to prove the part (i). Let Z be a closed complement of $\ker J$ in $\mathcal{X}$. Applying Theorem 3.3 and Remark 3.4 in Shi and Wang (2009) again, Λ^+ has one of the following three alternatives:

(a) Λ^+ meets another bifurcation point $(\bar{m}_a, 0, N_b, 0)$ with $\bar{m}_a \neq m_a^*$;
(b) Λ^+ includes a point $(m_a, \bar{A}(x), N_b + \bar{N}(x), \bar{C}(x))$ with $0 \neq (\bar{A}, \bar{N}, \bar{C}) \in Z$;
(c) Λ^+ is not compact in $\mathbb{R}^+ \times \mathcal{X}$.

If (a) holds, then we can find a positive solution sequence $\{(m_a^i, A_2^i, N_2^i, C_2^i)\}$ of (3.4) such that $(m_a^i, A_2^i, N_2^i, C_2^i) \to (\bar{m}_a, 0, N_b, 0)$ in $C([0, L])$ as $i \to \infty$. Let $\bar{a}_i = A_2^i / \|A_2^i\|_\infty$. Similar to those in the proof of part (2) in Lemma 3.4, we conclude that $\bar{a}_i \to \bar{a}$ and $\bar{a}$ satisfies

$$\begin{cases} D_a \bar{a}'' - v\bar{a}' + (r_a g(N_b) f(I(x, 0)) - \bar{m}_a)\bar{a} = 0, \ x \in (0, L), \\ D_a \bar{a}'(0) - v\bar{a}(0) = D_a \bar{a}'(L) - v\bar{a}(L) = 0. \end{cases} \quad (3.16)$$

Then, we obtain $\bar{a} > 0$ for all $x \in [0, L]$ since $\bar{a} \geq 0$ and $\|\bar{a}\|_\infty = 1$. It follows from (3.5) that

$$\bar{m}_a = \lambda_1(r_a g(N_b) f(I(x, 0)), D_a, v, L) = m_a^*.$$

This is a contradiction, hence the alternative (a) cannot happen.

If (b) holds, then $(\bar{A}, N_b + \bar{N}, \bar{C})$ is a positive solution of (3.4). It follows from Lemma 3.4 that $\bar{A} > 0$, $N_b + \bar{N} < N_b$ and $\bar{C} > 0$ for all $x \in [0, L]$. It follows from $(\bar{A}, \bar{N}, \bar{C}) \in Z$ that

$$Q = \int_0^L (\bar{A}(x)\bar{\zeta}(x) + \bar{N}(x)\bar{\varphi}(x) + \bar{C}(x)\bar{\psi}(x)) \mathrm{d}x = 0. \quad (3.17)$$

By $\bar{\zeta} > 0$, $\bar{\varphi} < 0$ and $\bar{\psi} > 0$, we have $Q > 0$, which contradicts with (3.17). Therefore, the alternative (b) cannot happen.

In view of the above discussion, the alternative (c) must happen, and Λ^+ is unbounded in $\mathbb{R}^+ \times \mathcal{X}$. According to Lemma 3.4, (3.4) has no nonnegative solution for $m_a > m_a^*$, and $(A_2(x), N_2(x), C_2(x))$ is bounded on $[0, L]$ when $m_a \in [\varepsilon, m_a^*]$ with any $\varepsilon > 0$. This shows that the projection of Λ^+ onto m_a-axis contains $(0, m_a^*)$. The proof of part (i) is complete. □

Remark 3.6   1. In Nie et al. (2020) and Nie et al. (2015), Nie et al. obtained the uniqueness of the positive steady-state solution for a predator–prey system and a nutrient–phytoplankton system, respectively. They used the degree theory and some novel mathematical techniques. In this study, we cannot get any results for the uniqueness of E_2 in theory. This is because that (3.4) has a nonlocal term $f(I(x, A))$, which makes it difficult to apply the methods and techniques in Nie et al. (2020) and Nie et al. (2015). The numerical simulations show that E_2 is not only unique for $R_a > 1$, but also globally asymptotically stable if $R_b < 1$. This is an open question for future mathematical development.

2. It is obvious that R_a is a strictly increasing function for N_b and I_{in}. From Theorems 3.2–3.9 in Hsu and Lou (2010), R_a is strictly decreasing for v and L. Therefore, high I_{in} and N_b are conducive to the survival of algae, while large subsidence rate v and increased water depth L can cause the extinction of algae. The influence of vertical turbulent diffusivity D_a on R_a is complex. Multiple critical thresholds of turbulent diffusivity may exist for algal persistence and extirpation.

3.3 Coexistence Steady States

From model (2.5), a coexistence steady-state solution $E_3 = (A_3(x), B_3(x), N_3(x), C_3(x))$ satisfies

$$
\begin{cases}
D_a A'' - v A' + r_a g(N) f(I(x, A)) A - m_a A = 0, & x \in (0, L), \\
D_b B'' + r_b g_b(N, C) B - m_b B = 0, & x \in (0, L), \\
D_n N'' - c_a r_a g(N) f(I(x, A)) A - c_b r_b g_b(N, C) B = 0, & x \in (0, L), \\
D_c C'' + r_a (1 - g(N)) f(I(x, A)) A - \dfrac{1}{\delta} r_b g_b(N, C) B - \alpha C = 0, & x \in (0, L), \\
D_a A'(0) - v A(0) = D_a A'(L) - v A(L) = 0, \ B'(0) = B'(L) = 0, \\
N'(0) = 0, \ D_n N'(L) = a(N_b - N(L)), \ C'(0) = C'(L) = 0,
\end{cases}
\tag{3.18}
$$

and each part of E_3 is positive. We explore the existence of E_3 by using the theory of repellers and persistence in Magal and Zhao (2005), Smith and Zhao (2001) and Zhao (2003). The method used here is similar to the one used in the proofs of Theorems 3.1 and 4.1 in Hsu et al. (2017).

In order to obtain our results, we consider the algae–nutrient–organic carbon interaction model:

$$
\begin{cases}
\dfrac{\partial A(x, t)}{\partial t} = D_a \dfrac{\partial^2 A}{\partial x^2} - v \dfrac{\partial A}{\partial x} + r_a g(N) f(I(x, A)) A - m_a A, & x \in (0, L), \ t > 0, \\
\dfrac{\partial N(x, t)}{\partial t} = D_n \dfrac{\partial^2 N}{\partial x^2} - c_a r_a g(N) f(I(x, A)) A, & x \in (0, L), \ t > 0, \\
\dfrac{\partial C(x, t)}{\partial t} = D_c \dfrac{\partial^2 C}{\partial x^2} + r_a (1 - g(N)) f(I(x, A)) A - \alpha C, & x \in (0, L), \ t > 0, \\
D_a A_x(0, t) - v A(0, t) = D_a A_x(L, t) - v A(L, t) = 0, & t > 0, \\
N_x(0, t) = 0, \ D_n N_x(L, t) = a(N_b - N(L, t)), & t > 0, \\
C_x(0, t) = C_x(L, t) = 0, & t > 0.
\end{cases}
\tag{3.19}
$$

Define a function space

$$
\mathbb{V} := \{(v_1, v_2, v_3) \in C([0, L], \mathbb{R}^3) : v_i(x) \geq 0 \text{ on } [0, L], \ i = 1, 2, 3\}.
$$

The system (3.19) generates a semiflow $\Phi(t) : \mathbb{V} \to \mathbb{V}$ by

$$
\Phi(t)(v_0)(x) = (A(x, t, v_0), N(x, t, v_0), C(x, t, v_0)), \ x \in [0, L], \ t \geq 0,
$$

where $v_0 = (A_0, N_0, C_0) \in \mathbb{V}$. Let

$$
\mathbb{V}^* := \{(A, N, C) \in \mathbb{V} : A(\cdot) \not\equiv 0\}, \ \partial \mathbb{V}^* := \mathbb{V} \setminus \mathbb{V}^*
$$

and

$$\Upsilon_1 := \{v_0 \in \partial\mathbb{V}^* : \Phi(t)v_0 \in \partial\mathbb{V}^* \text{ for all } t \geq 0\}.$$

We first show that $\{(0, N_b, 0)\}$ is a uniform weak repeller for $\mathbb{V}^*$, that is, there exists a $\sigma_1 > 0$ satisfying

$$\limsup_{t \to \infty} \|\Phi(t)v_0 - (0, N_b, 0)\| \geq \sigma_1 \text{ for any } v_0 = (A_0, N_0, C_0) \in \mathbb{V}^*. \quad (3.20)$$

Lemma 3.7 *If $R_a > 1$, then $\{(0, N_b, 0)\}$ is a uniform weak repeller for $\mathbb{V}^*$.*

Proof By $R_a > 1$, there exists a $\varepsilon_1 > 0$ such that $R_a^{\varepsilon_1} = m_a^*/(m_a + \varepsilon_1) > 1$. It follows from (3.5) that $m_a^* - m_a - \varepsilon_1 > 0$ is the principal eigenvalue of

$$\lambda\zeta(x) = D_a\zeta''(x) - v\zeta'(x) + (r_a g(N_b)f(I(x, 0)) - m_a - \varepsilon_1)\zeta(x), \ x \in (0, L),$$
$$D_a\zeta'(0) - v\zeta(0) = D_a\zeta'(L) - v\zeta(L) = 0.$$

Let $\zeta^{\varepsilon_1}(x)$ be the corresponding positive eigenvalue function. By the continuity of g and f, we can find a $\sigma_1 > 0$ satisfying

$$g(N(x))f(I(x, A(x))) > g(N_b)f(I(x, 0)) - \varepsilon_1 \text{ for all } x \in [0, L] \quad (3.21)$$

if $\|(A, N) - (0, N_b)\| < \sigma_1$.

If (3.20) is not true, then there exists a $v_0 \in \mathbb{V}^*$ satisfying

$$\limsup_{t \to \infty} \|\Phi(t)v_0 - (0, N_b, 0)\| < \sigma_1. \quad (3.22)$$

This means that we can find a $T_1 > 0$ satisfying

$$\|(A(\cdot, t, v_0), N(\cdot, t, v_0)) - (0, N_b)\| < \sigma_1, \ t \geq T_1.$$

Combining (3.21) with the equation of A in (3.19) gives

$$\frac{\partial A(x, t)}{\partial t} \geq D_a\frac{\partial^2 A}{\partial x^2} - v\frac{\partial A}{\partial x} + (r_a g(N_b)f(I(x, 0)) - m_a - \varepsilon_1)A, \ x \in (0, L),$$
$$t \geq T_1, D_a A_x(0, t) - vA(0, t) = D_a A_x(L, t) - vA(L, t) = 0, \ t \geq T_1.$$

Note that $A(\cdot, T_1, v_0) \gg 0$. We choose $b_1 > 0$ satisfying $A(x, T_1, v_0) \geq b_1\zeta^{\varepsilon_1}(x)$ on $[0, L]$. By the comparison theorem of parabolic equation, we have

$$A(x, t, v_0) \geq b_1 e^{(m_a^* - m_a - \varepsilon_1)(t - T_1)}\zeta^{\varepsilon_1}(x) \text{ for any } x \in [0, L], \ t \geq T_1,$$

where $b_1 e^{(m_a^* - m_a - \varepsilon_1)(t - T_1)}\zeta^{\varepsilon_1}(x)$ is a solution of the following system:

$$\frac{\partial A(x, t)}{\partial t} = D_a\frac{\partial^2 A}{\partial x^2} - v\frac{\partial A}{\partial x} + (r_a g(N_b)f(I(x, 0)) - m_a - \varepsilon_1)A,$$

$x \in (0, L)$, $t \geq T_1$, $D_a A_x(0, t) - v A(0, t) = D_a A_x(L, t) - v A(L, t) = 0$, $t \geq T_1$,
$A(x, T_1) = b_1 \zeta^{\varepsilon_1}(x)$, $x \in [0, L]$.

Then, $\lim_{t \to \infty} A(\cdot, t, v_0) = \infty$ since $m_a^* - m_a - \varepsilon_1 > 0$. This is a contradiction to (3.22). Then, (3.20) holds. $\qquad \square$

We now prove that model (3.19) is uniformly persistent for $(\mathbb{V}^*, \partial \mathbb{V}^*)$, that is, there is a positive constant $\bar{\varepsilon} > 0$ satisfying

$$\liminf_{t \to \infty} A(\cdot, t, v_0) > \bar{\varepsilon} \quad \text{for any } v_0 \in \mathbb{V}^*.$$

Lemma 3.8 *If $R_a > 1$, then model (3.19) is uniformly persistent for $(\mathbb{V}^*, \partial \mathbb{V}^*)$. Moreover, $\Phi(t) : \mathbb{V}^* \to \mathbb{V}^*$ admits a global attractor Ω_0 with $\Omega_0 \subset \text{Int } \mathbb{V}$.*

Proof According to Theorem 3.1, $\Phi(t) : \mathbb{V} \to \mathbb{V}$ admits a global compact attractor in $\mathbb{V}$. Assume that $(A(x, t, v_0), N(x, t, v_0), C(x, t, v_0))$ is the solution of model (3.19) with the initial value $v_0 \in \mathbb{V}$. From the Hopf boundary lemma and strong maximum principle, we have

$$A(x, t, v_0) > 0 \text{ on } [0, L] \text{ for any } t > 0 \text{ and } v_0 \in \mathbb{V}^*. \tag{3.23}$$

Then, $\Phi(t)\mathbb{V}^* \subseteq \mathbb{V}^*$ for all $t \geq 0$.

We prove that the omega limit set $\omega(v_0) = \{(0, N_b, 0)\}$ of the orbit $o(v_0) := \{\Phi(t)v_0 : t \geq 0\}$ with the initial value $v_0 = (A_0, N_0, C_0) \in \Upsilon_1$. For any $v_0 \in \Upsilon_1$, we obtain $\Phi(t)v_0 \in \Upsilon_1$ for any $t \geq 0$, and then $A(\cdot, t, v_0) \equiv 0$. Then, the equation of C in (3.19) becomes

$$\frac{\partial C(x, t)}{\partial t} = D_c \frac{\partial^2 C}{\partial x^2} - \alpha C, \ x \in (0, L), \ C_x(0, t) = C_x(L, t) = 0, \ t > 0, \tag{3.24}$$

which implies that $\limsup_{t \to \infty} C(x, t) = 0$ on $[0, L]$. Then, (3.19) reduces to (3.11) and $N(x, t, v_0)$ converges to N_b uniformly on $[0, L]$ as $t \to \infty$. This indicates

$$\lim_{t \to \infty} (A(x, t, v_0), N(x, t, v_0), C(x, t, v_0)) = (0, N_b, 0) \text{ uniformly on } [0, L].$$

Now we establish the uniform persistence of model (3.19), and embed our problem in the frame of Theorem 3 in Smith and Zhao (2001). It follows from Lemma 3.7 that $\{(0, N_b, 0)\}$ is a uniform weak repeller with respect to $\mathbb{V}^*$. Let $\eta_1 : \mathbb{V} \to [0, \infty)$ be a continuous function and satisfy

$$\eta_1(v_0) := \min_{x \in [0,L]} A_0(x) \quad \text{for any } v_0 = (A_0, N_0, C_0) \in \mathbb{V}.$$

From the Hopf boundary lemma and strong maximum principle, we have $\eta_1^{-1}(0, \infty) \subseteq \mathbb{V}^*$ and $\eta_1(\Phi(t)v_0) > 0$ for any $t > 0$ if $\eta_1(v_0) > 0$ or $v_0 \in \mathbb{V}^*$ with $\eta_1(v_0) = 0$. Then, η_1 is a generalized distance function for the semiflow $\Phi(t) : \mathbb{V} \to \mathbb{V}$.

From the above analysis, we have the following conclusions: (i) any forward orbit of $\Phi(t)$ in Υ_1 converges to $(0, N_b, 0)$; (ii) no cycle from $(0, N_b, 0)$ to $(0, N_b, 0)$ in $\partial\mathbb{V}^*$; (iii) $(0, N_b, 0)$ is isolated in $\mathbb{V}$ and $W^s((0, N_b, 0)) \cap \mathbb{V}^* = \emptyset$, where $W^s((0, N_b, 0))$ is the stable set of $(0, N_b, 0)$. Note that $\Phi(t) : \mathbb{V} \to \mathbb{V}$ admits a global compact attractor in $\mathbb{V}$. From Theorem 3 in Smith and Zhao (2001), there exists a $\bar{\varepsilon} > 0$ such that $\min_{\varphi \in \omega(v_0)} \eta_1(\varphi) > \bar{\varepsilon}$ for any $v_0 \in \mathbb{V}^*$. This indicates that the uniform persistence of model (3.19) holds. It follows from Theorem 3.7 and Remark 3.10 in Magal and Zhao (2005) that $\Phi(t) : \mathbb{V}^* \to \mathbb{V}^*$ admits a global attractor Ω_0 in $\mathbb{V}^*$. Furthermore, $\Omega_0 \subset \text{Int } \mathbb{V}$ since (3.23) holds. This completes the proof. $\square$

Let

$$\mathbb{Y}^* := \{(A, B, N, C) \in \mathbb{Y} : A(\cdot) \not\equiv 0, \, B(\cdot) \not\equiv 0\} \text{ and } \partial\mathbb{Y}^* := \mathbb{Y} \setminus \mathbb{Y}^*,$$

where $\mathbb{Y}$ can be found in (3.3). Define a projection $\mathcal{T}$ on $\mathbb{V}$ by $\mathcal{T}(A, N, C) = (N, C)$ for any $(A, N, C) \in \mathbb{V}$ and let

$$\Theta_0 = \mathcal{T}(\Omega_0) \text{ and } \upsilon(x) = \inf_{(\phi_1^0, \phi_2^0) \in \Theta_0} g_b(\phi_1^0(x), \phi_2^0(x)) \text{ for any } x \in [0, L].$$

Here, Ω_0 can be found in Lemma 3.8. By Lemma 4.1 in Hsu et al. (2017), υ is continuous on $[0, L]$. We let $R_b^0 = m_b^0/m_b$, where $m_b^0 = \lambda_1(r_b \upsilon(x), D_b, L)$ is the principal eigenvalue of

$$\begin{aligned} \lambda\phi(x) &= D_b\phi''(x) + r_b\upsilon(x)\phi(x), \; x \in (0, L), \\ \phi'(0) &= \phi'(L) = 0. \end{aligned} \tag{3.25}$$

Assume that $M_0 := \{(A, 0, N, C) \in \mathbb{Y} : (A, N, C) \in \Omega_0\}$. The following lemmas show that E_1 and M_0 are uniform weak repellers, that is, there exist $\sigma_i > 0 \; (i = 2, 3)$ satisfying

$$\limsup_{t\to\infty} \text{dist}(\Pi(t)u_0, E_1) \geq \sigma_2$$

and

$$\limsup_{t\to\infty} \text{dist}(\Pi(t)u_0, M_0) \geq \sigma_3 \tag{3.26}$$

for all $u_0 = (A_0, B_0, N_0, C_0) \in \mathbb{Y}^*$.

Lemma 3.9 *If $R_a > 1$, then E_1 is a uniform weak repeller with respect to $\mathbb{Y}^*$.*

The proof of Lemma 3.9 is similar to the one for Lemma 3.7, thus we omit it here.

Lemma 3.10 *If $R_b^0 > 1$, then M_0 is a uniform weak repeller with respect to $\mathbb{Y}^*$.*

Proof It follows from $R_b^0 > 1$ that there is a $\varepsilon_2 > 0$ such that $R_b^{\varepsilon_2} = m_b^0/(m_b + \varepsilon_2) > 1$. By (3.25), $m_b^0 - m_b - \varepsilon_2 > 0$ is the principal eigenvalue of

$$\lambda\phi(x) = D_b\phi''(x) + (r_b\upsilon(x) - m_b - \varepsilon_2)\phi(x), \ x \in (0, L),$$
$$\phi'(0) = \phi'(L) = 0.$$

Let $\phi^{\varepsilon_2}(x)$ be the corresponding positive eigenvalue function. Note that Θ_0 is compact. For the above ε_2 and any $(\phi_1, \phi_2) \in C([0, 1], \mathbb{R}^2)$, there exists a $\sigma_3 > 0$ and $(\phi_1^*, \phi_2^*) \in \Theta_0$ with (ϕ_1^*, ϕ_2^*) depending on (ϕ_1, ϕ_2) such that

$$\text{dist}(g_b(\phi_1(\cdot), \phi_2(\cdot)), g_b(\Theta_0)) = \|g_b(\phi_1(\cdot), \phi_2(\cdot)) - g_b(\phi_1^*(\cdot), \phi_2^*(\cdot))\| < \varepsilon_2$$
$$(3.27)$$

if $\text{dist}((\phi_1(\cdot), \phi_2(\cdot)), \Theta_0) < \sigma_3$.

If (3.26) does not hold, then for the above $\sigma_3 > 0$, we can find a $u_0 \in \mathbb{Y}^*$ satisfying $\limsup_{t \to \infty} \text{dist}(\Pi(t)u_0, M_0) < \sigma_3$. This shows that

$$\limsup_{t \to \infty} \text{dist}((N(\cdot, t, u_0), C(\cdot, t, u_0)), \Theta_0) < \sigma_3, \qquad (3.28\text{a})$$

$$\limsup_{t \to \infty} \|B(\cdot, t)\| < \sigma_3. \qquad (3.28\text{b})$$

By (3.28a), there exists a $T_2 > 0$ satisfying

$$\text{dist}((N(\cdot, t, u_0), C(\cdot, t, u_0)), \Theta_0) < \sigma_3 \text{ for all } t \geq T_2.$$

From (3.27), there exists $(\phi_1^t, \phi_2^t) \in \Theta_0$ such that

$$\|g_b(N(\cdot, t, u_0), C(\cdot, t, u_0)) - g_b(\phi_1^t(\cdot), \phi_2^t(\cdot))\| < \varepsilon_2 \text{ for all } t \geq T_2.$$

Then,

$$g_b(N(\cdot, t, u_0), C(\cdot, t, u_0)) > g_b(\phi_1^t(\cdot), \phi_2^t(\cdot)) - \varepsilon_2 \geq \upsilon(\cdot) - \varepsilon_2$$

By (2.5), we have

$$\frac{\partial B(x, t)}{\partial t} \geq D_b \frac{\partial^2 B}{\partial x^2} + (r_b\upsilon(x) - m_b - \varepsilon_2)B, \ x \in (0, L), \ t \geq T_2,$$
$$B_x(0, t) = B_x(L, t) = 0, \ t \geq T_2.$$

Note that $B(\cdot, T_2, u_0) \gg 0$ since $u_0 \in \mathbb{Y}^*$. We can find a $b_2 > 0$ satisfying $B(x, T_2, u_0) \geq b_2\phi^{\varepsilon_2}(x)$ for all $x \in [0, L]$. From the comparison theorem of parabolic equation, we obtain

$$B(x, t, u_0) \geq b_2 e^{(m_b^0 - m_b - \varepsilon_2)(t - T_2)}\phi^{\varepsilon_2}(x) \text{ for all } x \in [0, L], \ t \geq T_2.$$

Then, we have $\lim_{t\to\infty} B(\cdot, t, u_0) = \infty$ since $m_b^0 - m_b - \varepsilon_2 > 0$. This contradicts (3.28b) and completes the proof. □

We next establish the existence of E_3 and state that model (2.5) is uniformly persistent for $(\mathbb{Y}^*, \partial\mathbb{Y}^*)$, that is, there is a positive constant $\tilde{\varepsilon} > 0$ satisfying

$$\liminf_{t\to\infty} A(\cdot, t, u_0) > \tilde{\varepsilon} \text{ and } \liminf_{t\to\infty} B(\cdot, t, u_0) > \tilde{\varepsilon} \text{ for any } u_0 \in \mathbb{Y}^*. \quad (3.29)$$

Theorem 3.11 *If $R_a > 1$ and $R_b^0 > 1$, then model (2.5) is uniformly persistent for $(\mathbb{Y}^*, \partial\mathbb{Y}^*)$. Moreover, model (2.5) has at least one coexistence steady-state solution E_3.*

Proof By the Hopf boundary lemma and strong maximum principle, we obtain

$$A(x, t, u_0) > 0, \ B(x, t, u_0) > 0 \text{ on } [0, L] \text{ for any } t > 0 \text{ and } u_0 \in \mathbb{Y}^*. \quad (3.30)$$

Then, $\Pi(t) : \mathbb{Y}^* \to \mathbb{Y}^*, t \geq 0$. Let

$$\Upsilon_2 := \{u_0 \in \partial\mathbb{Y}^* : \Pi(t)u_0 \in \partial\mathbb{Y}^* \text{ for all } t \geq 0\}.$$

We show that the omega limit set $\omega(u_0) \subset E_1 \cup M_0$ of the orbit $o(u_0) := \{\Pi(t)u_0 : t \geq 0\}$ with the initial value $u_0 = (A_0, B_0, N_0, C_0) \in \Upsilon_2$. For any fixed $u_0 \in \Upsilon_2$, we have $\Pi(t)u_0 \in \Upsilon_2$ for any $t \geq 0$ and consider the following three cases: (1) $A_0 \equiv 0, B_0 \equiv 0$; (2) $A_0 \equiv 0, B_0 \not\equiv 0$; (3) $A_0 \not\equiv 0, B_0 \equiv 0$.
Case (1): $A_0 \equiv 0, B_0 \equiv 0$. In this case, we have $A(\cdot, t, u_0) \equiv 0$ and $B(\cdot, t, u_0) \equiv 0$ for all $t \geq 0$. From (3.24) and (3.11), we obtain

$$\lim_{t\to\infty} (A(x, t, u_0), B(x, t, u_0), N(x, t, u_0), C(x, t, u_0)) = (0, 0, N_b, 0) \quad (3.31)$$

uniformly for $x \in [0, L]$.
Case (2): $A_0 \equiv 0, B_0 \not\equiv 0$. It follows that $A(\cdot, t, u_0) \equiv 0$ for all $t \geq 0$. By (3.9), (3.10) and (3.11), we conclude that (3.31) holds.
Case (3): $A_0 \not\equiv 0, B_0 \equiv 0$. In this case, $B(\cdot, t, u_0) \equiv 0$ for all $t \geq 0$. Then, (2.5) reduces to (3.19). By Lemma 3.8, $(A(\cdot, t, u_0), N(\cdot, t, u_0), C(\cdot, t, u_0))$ will converge and enter the global attractor $\Omega_0 \in \text{Int } \mathbb{V}$. This means that $\Pi(t)u_0$ will enter M_0 as $t \to \infty$, and $\omega(u_0) \subset M_0$.
Coupling cases (1)-(3), we have $\omega(u_0) \subset E_1 \cup M_0$ for any $u_0 \in \Upsilon_2$. By Lemmas 3.9 and 3.10, E_1 and M_0 are uniform weak repellers with respect to $\mathbb{Y}^*$.
We once again embed our problem in the frame of Theorem 3 in Smith and Zhao (2001). We define $\eta_2 : \mathbb{Y} \to [0, \infty)$ satisfying

$$\eta_2(u_0) := \min \left\{ \min_{x\in[0,L]} A_0(x), \min_{x\in[0,L]} B_0(x) \right\}$$

for any $u_0 = (A_0, B_0, N_0, C_0) \in \mathbb{Y}$. It follows from (3.30) that $\eta_2^{-1}(0, \infty) \subseteq \mathbb{Y}^*$ and $\eta_2(\Pi(t)u_0) > 0$ for any $t > 0$ if $\eta_2(u_0) > 0$ or $u_0 \in \mathbb{Y}^*$ with $\eta_2(u_0) = 0$. Hence,

η_2 is a generalized distance function for the semiflow $\Pi(t) : \mathbb{Y} \to \mathbb{Y}$. In light of the above discussion, we obtain the following conclusions: (i) $\omega(u_0) \subset E_1 \cup M_0$ for any $u_0 \in \Upsilon_2$; (ii) no subset of E_1, M_0 forms a cycle in Υ_2; (iii) E_1 and M_0 are isolated in $\mathbb{Y}$; (iv) $W^s(E_1) \cap \mathbb{Y}^* = \emptyset$ and $W^s(M_0) \cap \mathbb{Y}^* = \emptyset$, where $W^s(E_1)$ and $W^s(M_0)$ are the stable sets of E_1 and M_0, respectively. Note that $\Pi(t) : \mathbb{Y} \to \mathbb{Y}$ has a global compact attractor in $\mathbb{Y}$. We can find a $\tilde{\varepsilon} > 0$ such that $\min_{\phi \in \omega(u_0)} \eta_2(\phi) > \tilde{\varepsilon}$ for any $u_0 \in \mathbb{Y}^*$ (see Theorem 3 in Smith and Zhao 2001). This shows that (3.29) holds and model (3.19) is uniformly persistent for $(\mathbb{Y}^*, \partial \mathbb{Y}^*)$. From Theorem 3.7 and Remark 3.10 in Magal and Zhao (2005), $\Pi(t) : \mathbb{Y}^* \to \mathbb{Y}^*$ has a global attractor. Moreover, by Theorem 4.7 in Magal and Zhao (2005), model (2.5) has a coexistence steady-state solution $E_3 \in \mathbb{Y}^*$. From (3.18) and Lemma 3.4, $A_3(x) > 0$, $N_3(x) > 0$, $C_3(x) > 0$ on $[0, L]$. The second equation in (3.18) gives

$$-D_b B_3'' + m_b B_3 = r_b g_b(N_3, C_3) B_3 \geq 0, \ x \in (0, L), \ B_3'(0) = B_3'(L) = 0.$$

Then, $B_3 > 0$ on $[0, L]$ from the strong maximum principle. The proof is complete. $\qquad \square$

Remark 3.12 1. When $R_a > 1$ and $R_b^0 > 1$, Theorem 3.11 indicates that all populations can coexist. If $R_a > 1$ and $R_b < 1$, E_2 is globally asymptotically stable from numerical simulations. It can be easily seen that $M_0 = E_2$ and $R_b^0 = R_b$. This means that $R_b = 1$ is a critical value for bacteria from extirpation to survival.

2. In the theoretical analysis, we prove that algae and bacteria coexist in a positive steady-state solution. However, the form of their coexistence is complicated. It may also be a positive spatially inhomogeneous periodic solution from the following numerical simulations. How to prove the existence of periodic solutions is a question worthy of further study.

3.4 Simulations

According to ecologically reasonable parameter values (see Table 2), we do some numerical simulations to illustrate and supplement our above theoretical analysis. For different algal and bacterial loss rates m_a, m_b, Fig. 2 shows dynamic numerical simulations of solutions of (2.5). From Theorems 3.2, 3.5, 3.11 and parameter values in Table 2, the solutions of (2.5) converge to different steady states or a positive spatially inhomogeneous periodic solution regardless of initial conditions.

When $R_a = m_a^*/m_a = 0.91 < 1$ ($m_a^* = 0.91, m_a = 1$), one can observe that the extinction of both algae and bacteria is the outcome. At the same time, the dissolved nutrient concentration reaches the fixed external dissolved nutrient concentration N_b (see Theorem 3.2 and Fig. 2a$_1$–d$_1$). This happens because the large algal loss rate causes the extinction of algae. It in turn leads to the extinction of bacteria due to the bottom-up control of algae on bacteria. This also means that dissolved nutrients are distributed evenly in the case of algae extinction.

When $R_a = m_a^*/m_a = 9.1 > 1$ and $R_b = m_b^*/m_b = 0.186 < 1$ ($m_a^* = 0.91, m_a = 0.1, m_b^* = 0.52, m_b = 2.8$), algae, organic carbon and dissolved nutrients coexist in the poorly mixed aquatic environment (see Theorem 3.5 and Fig. 2a$_2$–d$_2$). In this

Table 2 Numerical values of parameters in model (2.5) with references

Symbol	Value	Unit	Source	Symbol	Value	Unit	Source
D_a, D_b, D_n, D_c	0.2 (0.01–10)	m²/day	(Grover 2017; Huisman et al. 2002, 2006; Jäger et al. 2010; Klausmeier and Litchman 2001; Ryabov et al. 2010)	v	0.1 (−0.2–0.5)	m/day	(Grover 2017; Huisman et al. 2002; Jäger et al. 2010; Jäger and Diehl 2014; Ryabov et al. 2010)
r_a	1.5	day⁻¹	(Vasconcelos et al. 2016)	r_b	3 (1.5–4)	day⁻¹	(Codeço and Grover 2001; Wang et al. 2007)
L	10	m	Assumption	I_{in}	300	µmol photons m⁻²s⁻¹	(Jäger and Diehl 2014; Wang et al. 2007)
K_{bg}	0.4 (0.1–1)	m⁻¹	(Jäger and Diehl 2014; Wang et al. 2007)	k	0.0003	m²/mg C	(Vasconcelos et al. 2016; Wang et al. 2007)
α	0.01	day⁻¹	Assumption	γ	100	µmol photons m⁻²s⁻¹	(Jäger and Diehl 2014)
β	3	mg P/m³	(Jäger and Diehl 2014; Vasconcelos et al. 2016)	c_a	0.015 (0.004–0.04)	mgP/mg C	(Jäger and Diehl 2014; Wang et al. 2007)
c_b	0.1	mgP/mg C	(Wang et al. 2007)	a	0.05	m/day	(Jäger and Diehl 2014; Vasconcelos et al. 2016)
N_b	120 (0.5–500)	mgP/m³	(Jäger and Diehl 2014; Wang et al. 2007)	δ	0.5 (0.31–0.75)	-	(Wang et al. 2007)
η_n	0.1 (0.06–0.4)	mgP/m³	(Codeço and Grover 2001; Wang et al. 2007)	η_c	250 (100–400)	mgC/m³	(Wang et al. 2007)
m_a	0.1	day⁻¹	(Jäger and Diehl 2014; Vasconcelos et al. 2016)	m_b	0.3 (0.01–0.36)	day⁻¹	(Edwards 2019; Wang et al. 2007)
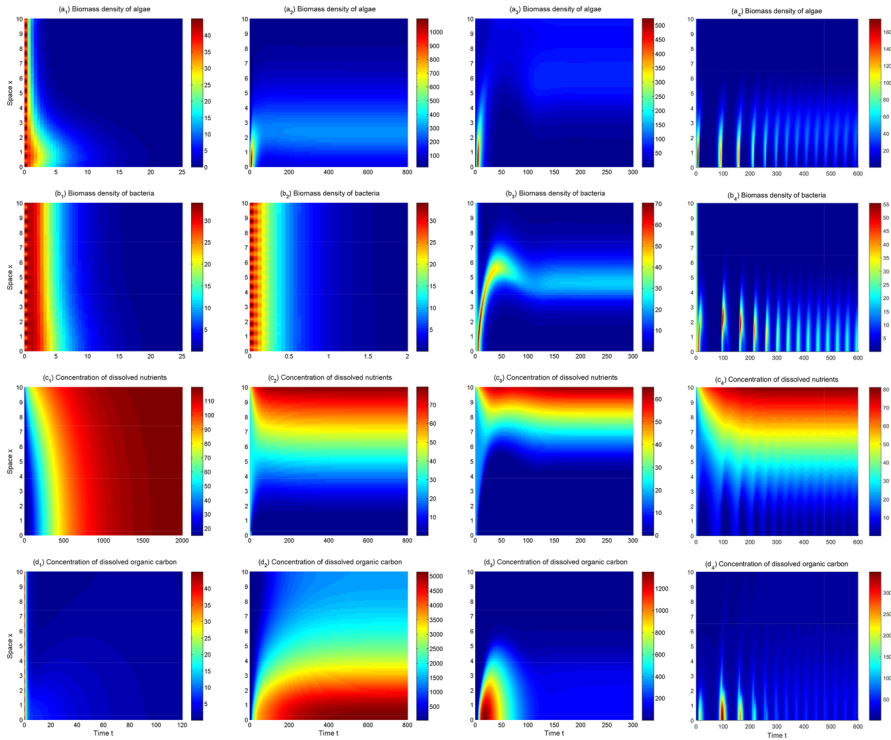
Fig. 2 ($\mathbf{a_1}$)–($\mathbf{d_1}$): The solution converges to E_1 with $m_a = 1$, $m_b = 0.3$; ($\mathbf{a_2}$)–($\mathbf{d_2}$): The solution converges to E_2 with $m_a = 0.1$, $m_b = 2.8$; ($\mathbf{a_3}$)–($\mathbf{d_3}$): The solution converges to E_3 with $m_a = 0.1$, $m_b = 0.3$; ($\mathbf{a_4}$)–($\mathbf{d_4}$): The solution converges to a positive spatially inhomogeneous periodic solution with $m_a = 0.5$, $m_b = 0.3$. Here the initial values are $A_0(x) = 40 + 5 \sin x$, $B_0(x) = 30 + 5 \cos x$, $N_0(x) = 30 + 4 \cos x$, $C_0(x) = 40 + 5 \sin x$ and other parameters are given in Table 2

situation, algae release a large amount of organic carbon through photosynthesis. Because there is no bacterial degradation considered, organic carbon accumulates, thereby forming organic carbon pollution in aquatic ecosystems. For $R_a > 1$ and $R_b < 1$, our numerical simulations show that all solutions of model (2.5) converge to E_2. This implies that E_2 is unique and globally asymptotically stable.

When $R_a = m_a^*/m_a = 9.1 > 1$ and $R_b = m_b^*/m_b = 1.73 > 1$ ($m_a^* = 0.91$, $m_a = 0.1$, $m_b^* = 0.52$, $m_b = 0.3$), model (2.5) is uniformly persistent and the solutions tend to the coexistence steady state E_3 (see Theorem 3.11 and Fig. 2a$_3$–d$_3$) or a positive spatially inhomogeneous periodic solution (see Fig. 2a$_4$–d$_4$). The periodic solution is generated by Hopf bifurcation at E_3. This also indicates that algae, bacteria, nutrients and organic carbon can appear together in a water column with positive levels. From Fig. 2, one can see that bacteria have two important functions. One function is that bacteria effectively degrade organic carbon, thereby reducing organic pollution (see Fig. 2d$_2$, d$_3$). The other function is that bacteria consume a lot of nutrients and cause a reduction in the algal biomass density through competition (see Fig. 2a$_2$, a$_3$). This reduces the probability of algal blooms. In Fig. 2, algae, bacteria and organic carbon also show strong spatial heterogeneity and vertical aggregation.

4 Biomass Density and Vertical Distribution of Algae or Bacteria

The algal biomass density and vertical distribution are two important indicators to evaluate algal blooms and measure the sustainable development of an aquatic ecosystem (Huisman et al. 2006; Klausmeier and Litchman 2001; Ryabov et al. 2010; Yoshiyama et al. 2009; Zhang et al. 2021a). They are influenced by spatial factors (turbulent diffusion and advection) and abiotic factors (nutrients and light) (Klausmeier and Litchman 2001; Ryabov et al. 2010; Zhang et al. 2021a). It is noted that algae have a bottom-up control on bacteria, and compete for nutrients with bacteria. This means that the algal biomass density and vertical distribution are correlated to the ones of bacteria. Therefore, in the following discussion, we will explore the influence of spatial factors and abiotic factors on the biomass density and vertical distribution of algae or bacteria in the poorly mixed aquatic environment. Especially, we will explore the important role of bacteria in the distribution and biomass changes of algae. The parameter values in the following figures are listed in Table 2.

In the following analysis, we consider the semi-trivial steady state $A_2(x)$ and the coexistence steady states $A_3(x)$, $B_3(x)$. In figures below, we compare the vertical distribution profiles of $A_2(x)$, $A_3(x)$ and $B_3(x)$ for different parameter choices. The numerical bifurcation diagrams show the change trend of spatial average biomass density of algae and bacteria for different parameter values when the solutions of model (2.5) converge to the steady states $A_2(x)$, $A_3(x)$, $B_3(x)$ or a positive spatially nonhomogeneous periodic solution.

We consider the influence of spatial factors including D_a, D_b, D_n, D_c and v on the algal or bacterial biomass density and vertical distribution. Here we assume that $D = D_a = D_b = D_n = D_c$. It is widely recognized that vertical turbulent diffusivity in an aquatic ecosystem varies significantly over seasons (Wüest and Lorke 2003). Figure 3 shows the vertical distribution of algae or bacteria for various values of turbulent diffusion rate D. One can observe that algal or bacterial biomass tends to be evenly distributed as D increases. This indicates that the large turbulent diffusion makes better mixing of algae and bacteria. The local maxima of the vertical distribution of algae and bacteria move upward since the large turbulent diffusion transports more nutrients to the water surface. It can also be noted that there are two algal accumulating layers in the water column for $D = 0.05$ under the asymmetric supply of nutrients from the water bottom and light from the water surface. This implies that there may be one or more Deep Chlorophyll Maxima (DCMs) in the poorly mixed aquatic reservoir.

In Fig. 4, one can see the changes of spatial average biomass density of algae and bacteria with respect to D when the solutions of model (2.5) converge to the steady states $A_2(x)$, $A_3(x)$, $B_3(x)$ or a positive spatially nonhomogeneous periodic solution. The algal biomass rises with the increase in D due to the improvement of nutrient transport in the case of bacterial extinction (see Fig. 4a). From Fig. 4b, the algal biomass exhibits complex changes in the case of bacterial survival. The increase in D first leads to a decrease in the algal biomass, and then causes periodic oscillations over time. There exists a bifurcating value D^* such that the system (2.5) undergoes a Hopf bifurcation at $D = D^*$ near E_3 and the bifurcating periodic solutions from $D = D^*$ are spatially nonhomogeneous. This is mainly caused by the complex relationship
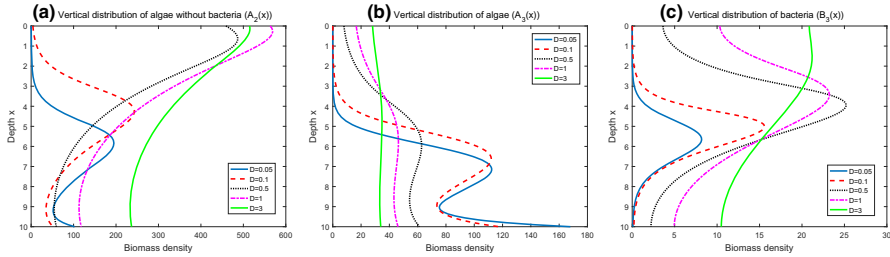
Fig. 3 Influence of the turbulent diffusion D ($D = D_a = D_b = D_n = D_c$) on the algal or bacterial vertical distribution. **a**: Vertical distribution profiles of the steady state $A_2(x)$ for varying D when bacteria are extinct; **b**, **c** Vertical distribution profiles of the steady states $A_3(x)$ and $B_3(x)$ for varying D. The horizontal axis is the biomass density coordinate of algae or bacteria, and the vertical axis is the depth coordinate of the water column
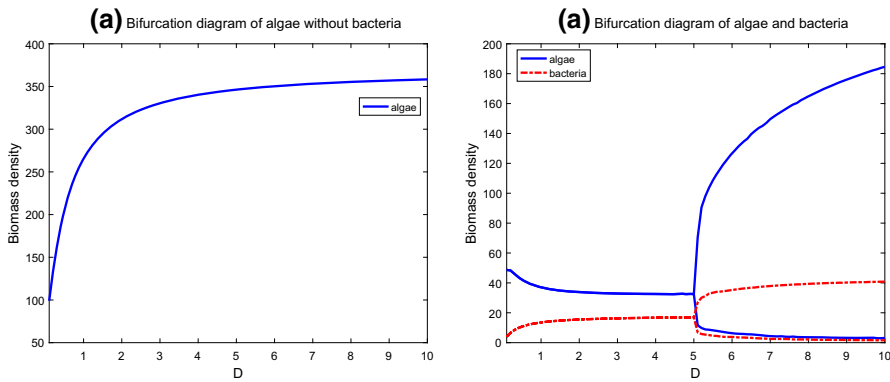
Fig. 4 Influence of the turbulent diffusion $D \in (0.01, 10)$ on the biomass density of algae or bacteria. **a** Spatial average biomass density of algae without bacteria for varying D when the solutions of model (2.5) converge to the steady state $A_2(x)$; **b** spatial average biomass density of algae and bacteria for varying D when the solutions of model (2.5) converge to the steady states $A_3(x)$, $B_3(x)$ or a positive spatially nonhomogeneous periodic solution

including a bottom-up control and competition between algae and bacteria (see Fig. 1).

The sign of advection rate v describes algal floating or sinking. In Fig. 5, one can see the transformation of algal aggregation for various values of advection rate v. An increase in v causes the local maxima of the algal vertical distribution to move downward, but the vertical distribution of bacteria does not change significantly. The algal biomass density reveals an increasing trend, while the bacterial biomass density remains almost unchanged (see Fig. 6). When bacteria survive, it is again observed that there is a bifurcating value v^* such that the system (2.5) undergoes a Hopf bifurcation at $v = v^*$ near E_3 (see Fig. 6b). The above discussion shows that v causes changes in algal vertical distribution and biomass, but has no effect on bacteria.

Abiotic factors such as nutrients and light are constantly changing over time and space. Here we consider four important environmental parameters related to light and nutrients: I_{in}, K_{bg}, N_b, and c_a. The light intensity at the surface I_{in} varies over seasons,
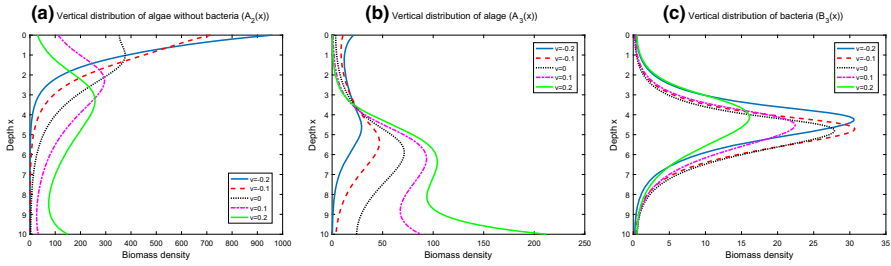
Fig. 5 Influence of the sinking or buoyant velocity v on the algal or bacterial vertical distribution
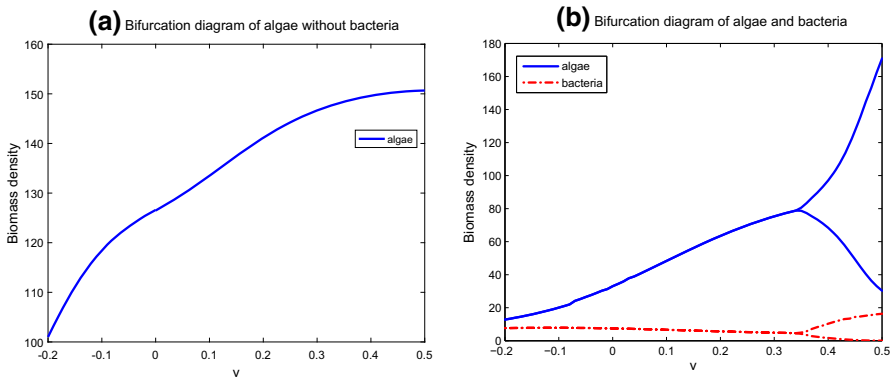
Fig. 6 Influence of the sinking or buoyant velocity $v \in (-0.2, 0.5)$ on the biomass density of algae or bacteria
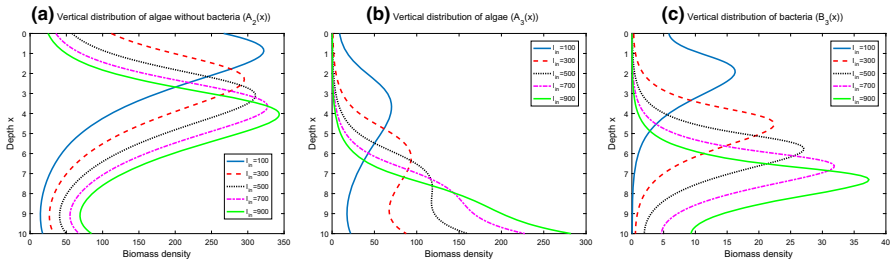
Fig. 7 Influence of the light intensity I_{in} on the algal or bacterial vertical distribution

and the background light attenuation coefficient K_{bg} describes the transmittance of water quality. In the absence of bacteria, algae mainly gather on the water surface for low I_{in} or high K_{bg}, while algae mainly gather in the middle of the water column for high I_{in} or low K_{bg} (see Figs. 7a, 8a). In the presence of bacteria, algae gradually concentrate toward the water bottom for I_{in} from low to high or K_{bg} from high to low (see Figs. 7b, 8b). Bacteria also show a similar trend for varying I_{in} or K_{bg} (see Figs. 7c, 8c). Therefore, high water surface light intensity or good water transmittance is conducive to the movement of algae to the water bottom.
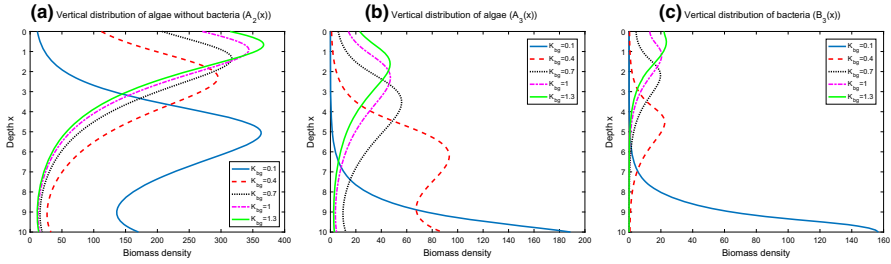
Fig. 8 Influence of the background light attenuation coefficient K_{bg} on the algal or bacterial vertical distribution
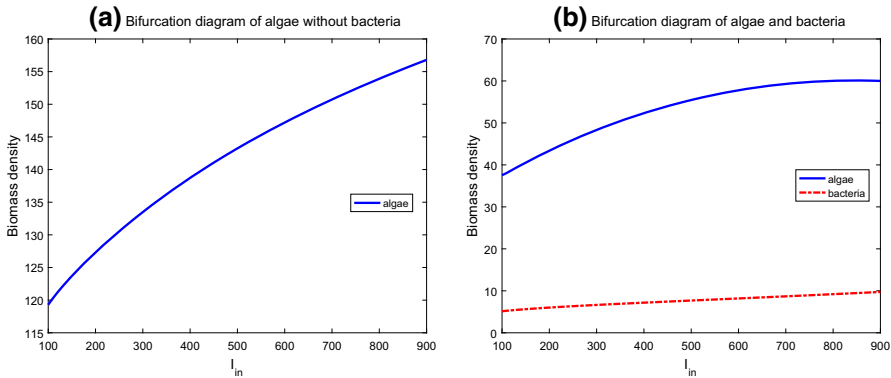
Fig. 9 Influence of the light intensity $I_{in} \in (100, 900)$ on the biomass density of algae or bacteria

In Fig. 9, one can observe that the increase in I_{in} is conducive to the algal and bacterial growth, resulting in the increase in their biomass. But the increase in bacterial biomass is relatively small because of the competition with algae for nutrients. If the light transmittance of water gradually deteriorates, the algal biomass decreases in the absence of bacteria (see Fig. 10a). The algal biomass exhibits a complex change trend for varying K_{bg} when bacteria invade the aquatic ecosystem. It first increases and then decreases, and finally shows periodic oscillations (see Fig. 10b). The biomass of bacteria keeps decreasing with the increase in K_{bg}, and also produces periodic oscillations. These are mainly attributed to the control and competition relationship between algae and bacteria. It is observed that the biomass density of algae decreases significantly after bacteria successfully invade the aquatic ecosystem (see Figs. 9, 10).

The nutrient input concentration N_b is closely related to the eutrophication of the water body. The average algal cell quota c_a describes the degree of algal growth requiring nutrients, and is an important index for evaluating the algal quality. If bacteria become extinct, high N_b or low c_a causes algae to accumulate on the water surface (see Figs. 11a, 12a). It is easy to induce harmful algal blooms. If algae and bacteria coexist, they mainly gather in the middle of the water column for varying N_b or c_a (see Figs. 11b, c and 12b, c). Figure 13 shows that the biomass density of algae and bacteria increases significantly with the increase in N_b. This is because the abundance of nutrients weakens competition between algae and bacteria. On the contrary, the increase in c_a causes the decrease in their biomass densities (see Fig. 14).
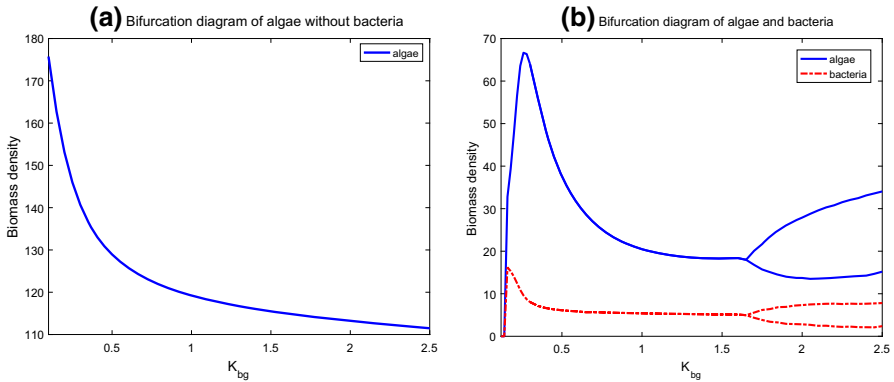
Fig. 10 Influence of the background light attenuation coefficient $K_{bg} \in (0.1, 2.5)$ on the biomass density of algae or bacteria
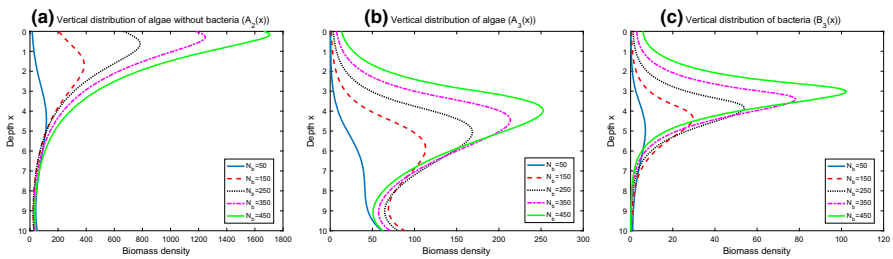
Fig. 11 Influence of the nutrient input concentration N_b on the algal or bacterial vertical distribution
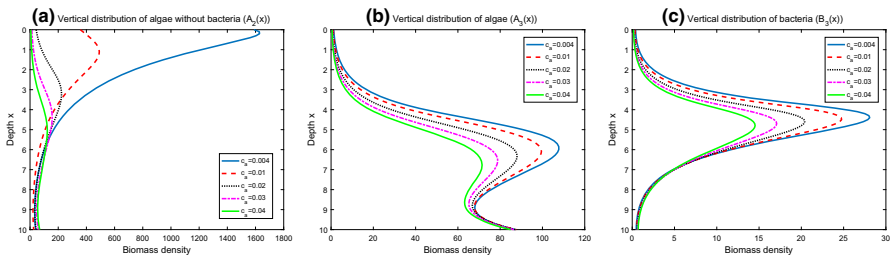
Fig. 12 Influence of the algal cell quota c_a on the algal or bacterial vertical distribution

The algal biomass density and vertical distribution are significantly different in the absence or presence of bacteria. If algae and bacteria coexist, it can be seen from the above figures that algae have a lower biomass density and are mainly concentrated in the middle and lower parts of the water column. The reason for this phenomenon is the competition between algae and bacteria for nutrients. When bacteria are extirpated, if nutrients are adequate or fully transmitted in the water column, algae move to the water surface with strong light in order to seek the optimal growth position, and then gather in the upper layer. When bacteria persist, they compete with algae for nutrients. This means that the local maxima of the algal and bacterial vertical distribution are located at different water depths. Due to the strong water surface light intensity, organic carbon
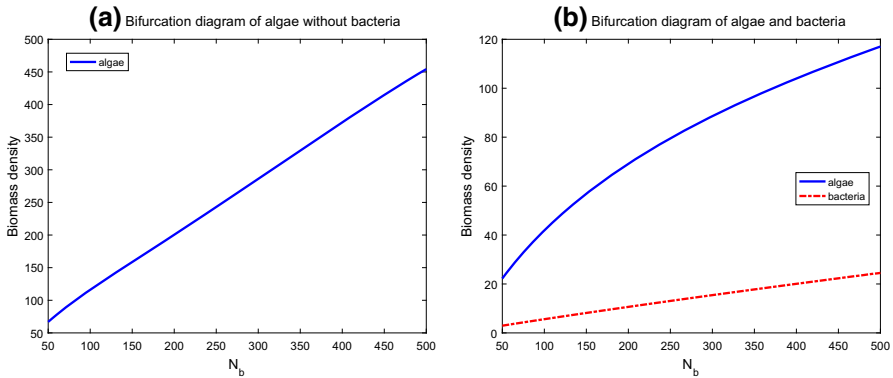
Fig. 13 Influence of the nutrient input concentration $N_b \in (50, 500)$ on the biomass density of algae or bacteria
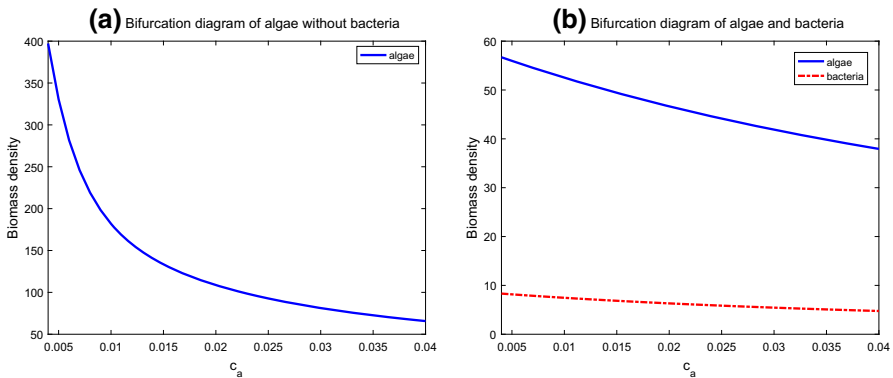
Fig. 14 Influence of the algal cell quota $c_a \in (0.004, 0.04)$ on the biomass density of algae or bacteria

is abundant in the upper part of the water column (see Fig. 2d$_2$, d$_3$). This makes bacteria have an advantage in the competition with algae, thus bacteria are more concentrated in the upper layer. Conversely, in the lower part of the water column, nutrients are richer but organic carbon is less rich, so algae dominate and mainly gather in the lower layer. These findings show that bacteria can effectively reduce the probability of harmful algal blooms.

5 Discussion

Algae have a bottom-up control on bacteria and compete with bacteria for nutrients. Their complex relationship has an important impact on the structure and sustainable development of aquatic communities (Crane and Grover 2010; Edwards 2019; Medina-Sánchez et al. 2004). We mechanistically formulate the model (2.5) to characterize the algae–bacteria dynamics in a poorly mixed aquatic environment. The basic ecological reproductive indices R_a, R_b for the invasion of algae and bacteria into aquatic

ecosystems are rigorously derived. All possibilities for the algal and bacterial survival and extinction are obtained with proofs.

Theoretical analysis shows that algae and bacteria go extinct if $R_a < 1$. The coexistence of algae, dissolved nutrients, and organic carbon is the outcome if $R_a > 1$ and $R_b < 1$. If $R_a > 1$ and $R_b > 1$, algae and bacteria coexist in two forms: a steady-state or a spatially inhomogeneous periodic solution. At this time, model (2.5) is uniformly persistent. The numerical simulations suggest that algae and bacteria exhibit strong spatial heterogeneity in a poorly mixed aquatic reservoir. They have complex vertical distribution and aggregation phenomena for different values of spatial parameters (D and v) and abiotic parameters (I_{in}, K_{bg}, N_b, and c_a).

In the existing algae–bacteria interaction models, the degradation of organic carbon by bacteria and the bottom-up control of bacteria by algae were mainly considered (Chang et al. 2021; Crane and Grover 2010; Edwards 2019; Kong et al. 2018; Yan et al. 2022). But it ignored the competition for nutrients between algae and bacteria. Our studies indicate that bacteria can effectively reduce the biomass of algae and prevent them from moving to the water surface due to the competitive effect. This shows that bacteria can reduce the possibility of algal blooms, especially in some oligotrophic aquatic environments. The phenomenon has not been noticed in previous studies. Therefore, it is a novel observation and can guide future management policies for controlling harmful algal blooms.

It is extremely challenging to obtain the complete dynamics of model (2.5) since it contains a nonlocal predator–prey structure within a high-dimensional system of partial differential equations. In the present paper, we explore steady-state solutions and the dissipation of the solutions. Nevertheless, there are still remaining dynamic properties of model (2.5) to be further investigated rigorously, for example, the existence of spatially nonhomogeneous periodic solutions and the stability of steady states E_2 and E_3.

Compared with the research work in Wang et al. (2007), our model considers the heterogeneity of the spatial distribution of algae and bacteria when the turbulence intensity is relatively weak. This spatial heterogeneity has been confirmed to be widely prevalent in aquatic ecosystems (Huisman et al. 2006; Klausmeier and Litchman 2001; Yoshiyama et al. 2009). In model (2.5), we do not consider the competitive relationship between bacterial strains under severely phosphorus limitation as in Wang et al. (2007). The reason is that the principal aim of this study is to model algae–bacteria interactions in a poorly mixed aquatic environment, and attempt to reveal the role of bacteria in algal blooms. The competition of bacterial strains is very important and affects the structure of aquatic communities. It will be of interest to contain the competing bacterial strains in model (2.5), and examine the Nishimura's hypothesis in Lake Biwa.

Here we take the average nutrient:carbon ratio in algae cells and ignore its change. It has been shown that algae have varying nutrient:carbon ratios, which have important implications in various aquatic ecological mechanisms (Davies and Wang 2021; Loladze et al. 2000; Wang et al. 2008). The relaxation of the relevant "strict homeostasis" assumption was mechanistically examined in Wang et al. (2012, 2018). A natural question is to explore how to reasonably introduce ecological stoichiometry into model (2.5), which is extremely challenging as discussed in the last paragraph of a recent synthesis paper (Wang et al. 2022).

From model (2.5) and the above discussion, there are more biological problems worthy of further exploration. Mixotrophic algae as the combination of autotroph and heterotroph synthesize organic matter through photosynthesis, and ingest bacteria to supply their own growth. It improves carbon fixation and effectively controls bacteria (Edwards 2019; Medina-Sánchez et al. 2004; Yan et al. 2022). Our model (2.5) does not consider the influence of mixotrophic algae on bacteria. It is worthwhile to further study mixotrophic algae–bacteria interactions in a poorly mixed aquatic reservoir. Carbon dioxide is an essential resource for algal photosynthesis (Davies and Wang 2021; Nie et al. 2016; Zhang et al. 2021b). Based on the research motivation of this paper, we ignore the effect of carbon dioxide in model (2.5). It would be insightful to incorporate carbon dioxide into model (2.5) as future study.

References

Chang, X.Y., Shi, J.P., Wang, H.: Spatial modeling and dynamics of organic matter biodegradation in the absence or presence of bacterivorous grazing. Math. Biosci. **331**, 108501 (2021)

Codeço, C.T., Grover, J.P.: Competition along a spatial gradient of resource supply: a microbial experimental model. Am. Nat. **157**(3), 300–315 (2001)

Crandall, M.G., Rabinowitz, P.H.: Bifurcation from simple eigenvalues. J. Funct. Anal. **8**(2), 321–340 (1971)

Crane, K.W., Grover, J.P.: Coexistence of mixotrophs, autotrophs, and heterotrophs in planktonic microbial communities. J. Theor. Biol. **262**(3), 517–527 (2010)

Davies, C.M., Wang, H.: Incorporating carbon dioxide into a stoichiometric producer-grazer model. J. Math. Biol. **83**, 49 (2021)

Du, Y.H., Hsu, S.B.: On a nonlocal reaction–diffusion problem arising from the modeling of phytoplankton growth. SIAM J. Math. Anal. **42**(3), 1305–1333 (2010)

Edwards, K.F.: Mixotrophy in nanoflagellates across environmental gradients in the ocean. Proc. Natl. Acad. Sci. USA **116**(13), 6211–6220 (2019)

Grover, J.P.: Sink or swim? Vertical movement and nutrient storage in phytoplankton. J. Theor. Biol. **432**(7), 38–48 (2017)

Hale, J.K.: Asymptotic Behavior of Dissipative Systems. American Mathematical Society, Providence (1988)

Heggerud, C.M., Wang, H., Lewis, M.A.: Transient dynamics of a stoichiometric cyanobacteria model via multiple-scale analysis. SIAM J. Appl. Math. **80**(3), 1223–1246 (2020)

Hsu, S.B., Lou, Y.: Single phytoplankton species growth with light and advection in a water column. SIAM J. Appl. Math. **70**(8), 2942–2974 (2010)

Hsu, S.B., Wang, F.B., Zhao, X.Q.: A reaction–diffusion model of harmful algae and zooplankton in an ecosystem. J. Math. Anal. Appl. **451**(2), 659–677 (2017)

Huisman, J., Weissing, F.J.: Light-limited growth and competition for light in well-mixed aquatic environments: an elementary model. Ecology **75**(2), 507–520 (1994)

Huisman, J., Arrayás, M., Ebert, U., Sommeijer, B.: How do sinking phytoplankton species manage to persist? Am. Nat. **159**(3), 245–254 (2002)

Huisman, J., Pham Thi, N.N., Karl, D.M., Sommeijer, B.: Reduced mixing generates oscillations and chaos in the oceanic deep chlorophyll maximum. Nature **439**, 322–325 (2006)

Jäger, C.G., Diehl, S.: Resource competition across habitat boundaries: asymmetric interactions between benthic and pelagic producers. Ecol. Monogr. **84**(2), 287–302 (2014)

Jäger, C.G., Diehl, S., Emans, M.: Physical determinants of phytoplankton production, algal stoichiometry, and vertical nutrient fluxes. Am. Nat. **175**(4), 91–104 (2010)

Klausmeier, C.A., Litchman, E.: Algal games: the vertical distribution of phytoplankton in poorly mixed water columns. Limnol. Oceanogr. **46**(8), 1998–2007 (2001)

Kong, J.D., Salceanu, P., Wang, H.: A stoichiometric organic matter decomposition model in a chemostat culture. J. Math. Biol. **76**(3), 609–644 (2018)

Loladze, I., Kuang, Y., Elser, J.J.: Stoichiometry in producer-grazer systems: linking energy flow with element cycling. Bull. Math. Biol. **62**, 1137–1162 (2000)

Magal, P., Zhao, X.Q.: Global attractors and steady states for uniformly persistent dynamical systems. SIAM J. Math. Anal. **37**(1), 251–275 (2005)

Medina-Sánchez, J.M., Villar-Argaiz, M., Carrillo, P.: Neither with nor without you: a complex algal control on bacterioplankton in a high mountain lake. Limnol. Oceanogr. **49**(5), 1722–1733 (2004)

Mei, L.F., Wang, F.B.: Dynamics of phytoplankton species competition for light and nutrient with recycling in a water column. Discrete Contin. Dyn. Syst. Ser. B **26**(4), 2115–2132 (2021)

Mischaikow, K., Smith, H., Thieme, H.R.: Asymptotically autonomous semiflows: chain recurrence and Lyapunov functions. Trans. Am. Math. Soc. **347**(5), 1669–1685 (1995)

Nie, H., Hsu, S.B., Wu, J.H.: Coexistence solutions of a competition model with two species in a water column. Discrete Contin. Dyn. Syst. Ser. B **20**(8), 2691–2714 (2015)

Nie, H., Hsu, S.B., Grover, J.P.: Algal competition in a water column with excessive dioxide in the atmosphere. J. Math. Biol. **72**(7), 1845–1892 (2016)

Nie, H., Wang, B., Wu, J.H.: Invasion analysis on a predator-prey system in open advective environments. J. Math. Biol. **81**(6), 1429–1463 (2020)

Pao, C.V.: Nonlinear Parabolic and Elliptic Equations. Plenum Press, New York (1992)

Ryabov, A.B., Rudolf, L., Blasius, B.: Vertical distribution and composition of phytoplankton under the influence of an upper mixed layer. J. Theor. Biol. **263**(1), 120–133 (2010)

Shi, J.P., Wang, X.F.: On global bifurcation for quasilinear elliptic systems on bounded domains. J. Differ. Equ. **246**(7), 2788–2812 (2009)

Smith, H.L., Zhao, X.Q.: Robust persistence for semidynamical systems. Nonlinear Anal. **47**(9), 6169–6179 (2001)

Thieme, H.R.: Convergence results and a Poincaré–Bendixson trichotomy for asymptotically autonomous differential equations. J. Math. Biol. **30**(7), 755–763 (1992)

Vasconcelos, F.R., Diehl, S., Rodríguez, P., Hedström, P., Karlsson, J., Byström, P.: Asymmetrical competition between aquatic primary producers in a warmer and browner world. Ecology **97**(10), 2580–2592 (2016)

Wang, H., Smith, H.L., Kuang, Y., Elser, J.J.: Dynamics of stoichiometric bacteria-algae interactions in the epilimnion. SIAM J. Appl. Math. **68**(2), 503–522 (2007)

Wang, H., Kuang, Y., Loladze, I.: Dynamics of a mechanistically derived stoichiometric producer-grazer model. J. Biol. Dyn. **2**(3), 286–296 (2008)

Wang, H., Sterner, R.W., Elser, J.J.: On the "strict homeostasis" assumption in ecological stoichiometry. Ecol. Model. **243**, 81–88 (2012)

Wang, H., Lu, Z., Raghavan, A.: Weak dynamical threshold for the "strict homeostasis" assumption in ecological stoichiometry. Ecol. Model. **384**, 233–240 (2018)

Wang, Y., Shi, J.P., Wang, J.F.: Persistence and extinction of population in reaction–diffusion–advection model with strong Allee effect growth. J. Math. Biol. **78**(7), 2093–2140 (2019)

Wang, H., Garcia, P.V., Ahmed, S., Heggerud, C.M.: Mathematical comparison and empirical review of the Monod and Droop forms for resource-based population dynamics. Ecol. Model. **466**, 109887 (2022)

Wüest, A., Lorke, A.: Small-scale hydrodynamics in lakes. Annu. Rev. Fluid Mech. **35**(1), 373–412 (2003)

Yan, Y.W., Zhang, J.M., Wang, H.: Dynamics of stoichiometric autotroph–mixotroph–bacteria interactions in the epilimnion. Bull. Math. Biol. **84**, 5 (2022)

Yoshiyama, K., Mellard, J.P., Litchman, E., Klausmeier, C.A.: Phytoplankton competition for nutrients and light in a stratified water column. Am. Nat. **174**(2), 190–203 (2009)

Zhang, J.M., Kong, J.D., Shi, J.P., Wang, H.: Phytoplankton competition for nutrients and light in a stratified lake: a mathematical model connecting epilimnion and hypolimnion. J. Nonlinear Sci. **31**, 35 (2021a)

Zhang, J.M., Shi, J.P., Chang, X.Y.: A model of algal growth depending on nutrients and inorganic carbon in a poorly mixed water column. J. Math. Biol. **83**, 15 (2021b)

Zhao, X.Q.: Dynamical Systems in Population Biology. Springer, New York (2003)